AGU PUBLICATIONS

JGR

Journal of Geophysical Research: Solid Earth

RESEARCH ARTICLE

10.1002/2014JB011779

Key Points:

- First Caribbean-wide, present-day, kinematic model
- Strain accumulation rates on all major active faults in the Caribbean
- Very low coupling on the Lesser Antilles-Puerto Rico subduction

Correspondence to:
E. Calais,
eric.calais@ens.fr

Citation:
Symithe, S., E. Calais, J. B. de Chabalier, R. Robertson, and M. Higgins (2015), Current block motions and strain accumulation on active faults in the Caribbean, *J. Geophys. Res. Solid Earth*, *120*, doi:10.1002/2014JB011779.

Received 16 NOV 2014
Accepted 24 MAR 2015
Accepted article online 28 APR 2015

Current block motions and strain accumulation on active faults in the Caribbean

S. Symithe[1], E. Calais[2], J. B. de Chabalier[3], R. Robertson[4], and M. Higgins[4]

[1]Department of Earth and Atmospheric Sciences, Purdue University, West Lafayette, Indiana, USA, [2]Ecole Normale Supérieure, Department of Geosciences, PSL Research University, UMR CNRS 8538, Paris, France, [3]Institut de Physique du Globe, Paris, France, [4]Seismic Research Center, University of the West Indies, St. Augustine, Trinidad and Tobago

Abstract The Caribbean plate and its boundaries with north and south America, marked by subduction and large intra-arc strike-slip faults, are a natural laboratory for the study of strain partitioning and interseismic plate coupling in relation to large earthquakes. Here we use most of the available campaign and continuous GPS measurements in the Caribbean to derive a regional velocity field expressed in a consistent reference frame. We use this velocity field as input to a kinematic model where surface velocities results from the rotation of rigid blocks bounded by locked faults accumulating interseismic strain, while allowing for partial locking along the Lesser Antilles, Puerto Rico, and Hispaniola subduction. We test various block geometries, guided by previous regional kinematic models and geological information on active faults. Our findings refine a number of previously established results, in particular slip rates on the strike-slip faults systems bounding the Caribbean plate to the north and south, and the kinematics of the Gonave microplate. Our much-improved GPS velocity field in the Lesser Antilles compared to previous studies does not require the existence of a distinct Northern Lesser Antilles block and excludes more than 3 mm/yr of strain accumulation on the Lesser Antilles-Puerto Rico subduction plate interface, which appears essentially uncoupled. The transition from a coupled to an uncoupled subduction coincides with a transition in the long-term geological behavior of the Caribbean plate margin from compressional (Hispaniola) to extensional (Puerto Rico and Lesser Antilles), a characteristics shared with several other subduction systems.

1. Introduction

Most of the seismic energy of our planet is released at subduction zones by earthquakes that occur either at the plate interface or on active faults in the overriding plate. It has long been thought that interplate coupling in such contexts—hence their seismogenic potential—depended for a large part on the age of the subducting plate [*Ruff and Kanamori*, 1980]. Recent large subduction earthquakes have shaken this paradigm, to the point that some now claim that all subduction have the capacity of generating megaearthquakes regardless of the age of the subducting crust [*McCaffrey et al.*, 2008]. The issue has therefore refocused on spatial and temporal variations of interplate coupling and how these may relate to asperities and barriers on the plate interface and to the deformation of the overriding plate [e.g., *Chlieh et al.*, 2011; *Wallace et al.*, 2012a].

For instance, recent results along the Chilean subduction indicate that lateral variations of interseismic coupling are correlated with the rupture areas of the Maule (2011, M_w8.8) and Valdivia (1960, M_w9.5) earthquakes, and with the frictional properties of the plate contact derived from fore-arc morphology [*Cubas et al.*, 2013]. Similarly, the Colombian subduction shows lateral variations of interseismic coupling correlated with large historical earthquakes and with the segmentation of the upper plate into continental slivers translating with respect to both the Nazca and South American plates [*Nocquet et al.*, 2014].

The subduction of the north American plate under the Caribbean plate (Figure 1) also shows lateral variations of interseismic coupling correlated with a segmentation of the tectonic regime along the arc [*Manaker et al.*, 2008]. Over a short distance, the plate boundary evolves from a frontal subduction (Lesser Antilles) with arc-parallel extension to a very oblique subduction (Puerto Rico) with little deformation of the arc, and to a subduction-collision (Hispaniola) with large strike-slip faults in the overriding plate and an active mountain range culminating at 3300 m (Pico Duarte, Dominican Republic). Interestingly, the large historical earthquakes that struck the Lesser Antilles subduction may not be interplate events [*Stein et al.*, 1982], while those appear to concentrate in the north at the Hispaniola collision.

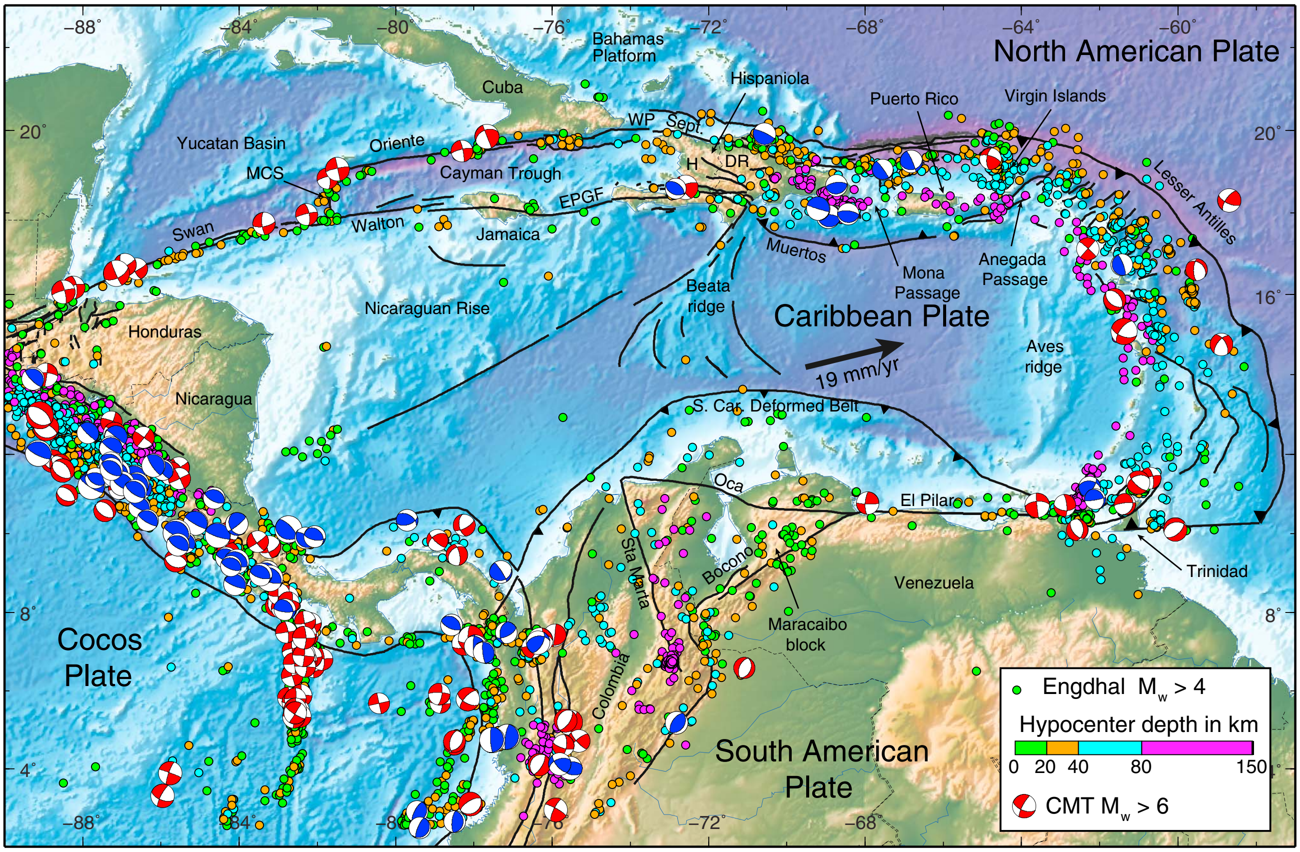

Figure 1. Seismotectonic setting of the Caribbean region. Black lines show the major active plate boundary faults. Colored circles are precisely relocated seismicity [1960–2008, *Engdahl et al.*, 1998] color coded as a function of depth. Earthquake focal mechanism are from the Global CMT Catalog (1976–2014) [*Ekstrom et al.*, 2012], thrust focal mechanisms are shown in blue, others in red. H = Haiti, DR = Dominican Republic, MCS = mid-Cayman spreading center, WP = Windward Passage, EPGF = Enriquillo Plaintain Garden fault.

The hypothesis has been put forward that this geological segmentation was correlated with interseismic coupling, reflecting the ability of the plate contact to transfer shear stress to the overriding plate [*Mann et al.*, 2002]. The segmentation would then also reflect the seismogenic capacity of the plate interface and possibly of the intra-arc faults. Here we test this hypothesis by jointly estimating interplate coupling and block kinematics in the whole Caribbean region east of 85°W. We also aim at providing a first-order kinematic description of surface deformation across the study area that can inform seismic hazard assessments and be compared with paleoseismological information. We do so using a new combined velocity field derived from campaign and continuous measurements at 300 sites, a 5 times increase since [*Manaker et al.*, 2008]. In particular, we include a new data set that significantly improves resolution in Puerto Rico and the Lesser Antilles and address the southern part of the Lesser Antilles subduction and the Caribbean plate boundary in South America.

2. Background

2.1. Tectonic Setting

The Caribbean domain and Central America form a small lithospheric plate inserted between North and South America (Figure 1). While the North and South American plates show little relative motion [*Patriat et al.*, 2011], the Caribbean plate moves eastward relative to them at 18–20 mm/yr [*DeMets et al.*, 2000]. This displacement is accommodated by two major east-north-east strike-slip fault systems along its northern boundary on either sides of the Cayman trough and at its southern boundary along the Oca-El Pilar fault system. The relative plate motion implies oblique convergence and subduction of the Atlantic oceanic lithosphere under the Greater Antilles (Hispaniola and Puerto Rico), transitioning to frontal subduction in the Lesser Antilles, then to pure strike-slip motion along the southern boundary of the Caribbean plate in South America. Plate boundary deformation at the Caribbean plate margins is accommodated by slip on a number of relatively well-identified

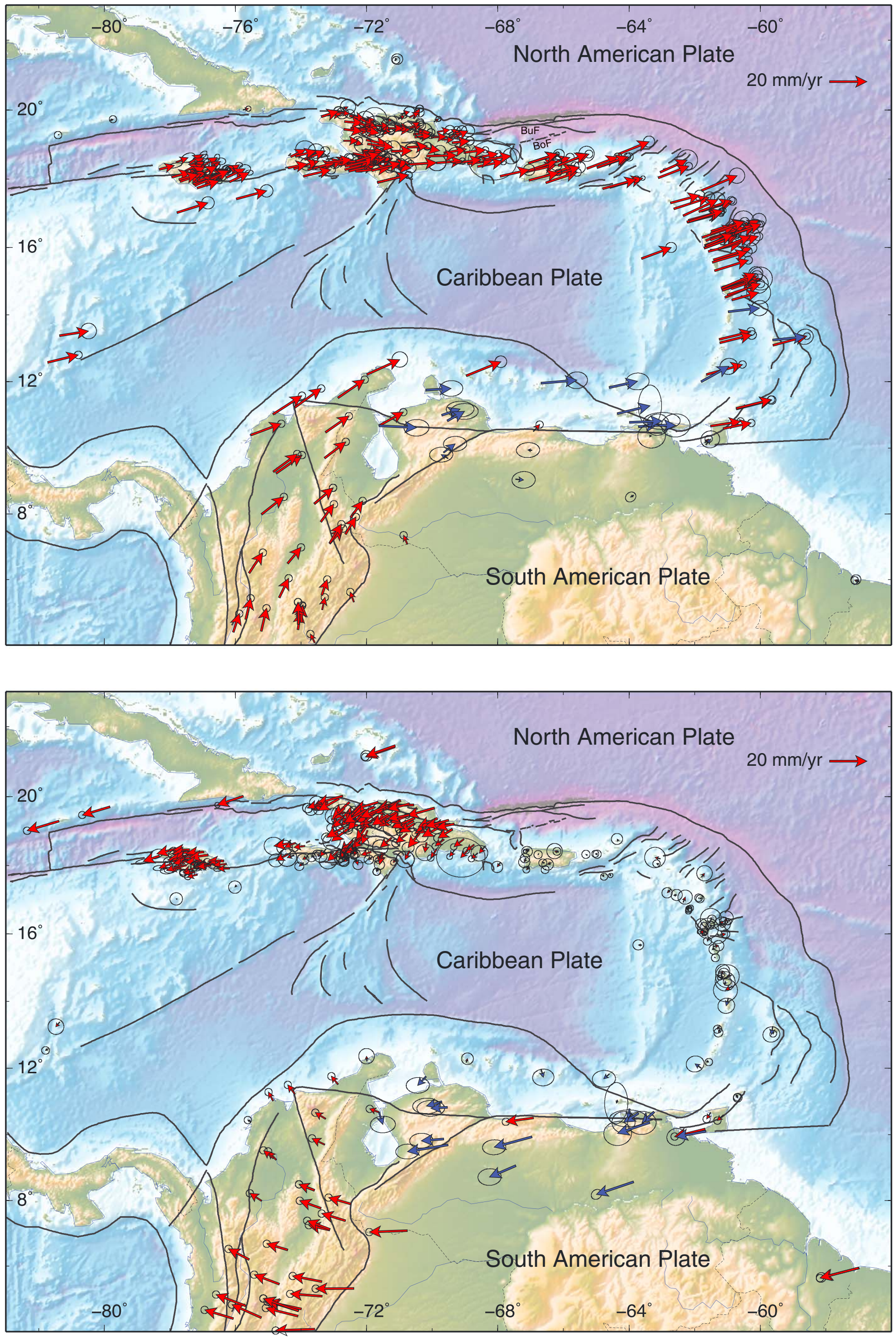

Figure 2. (top) GPS velocities used in the model shown with respect to the North American plate defined by the velocity of 25 GPS sites located in the stable interior of the plate [*Calais et al.*, 2006]. (bottom) GPS velocities shown with respect to the Caribbean plate as defined in the best fit block model described in the text. Error ellipses are 95% confidence. Blue arrows show GPS velocities from *Pérez et al.* [2001] in Venezuela because of their large uncertainty and the lack of common sites with our solution, which prevents us from rigorously combining them to our solution. They are not used in the model but used to show that they are consistent with the rest of the velocity field.

major faults. We briefly describe these structures thereafter as they will serve to define the geometry of our kinematic model.

At the northeastern edge of the study area (Figure 1), the Oriente fault bounds the Cayman trough, a 45 – 50 Ma oceanic pull apart basin [*Rosencrantz et al.*, 1988], to the north. Earthquake focal mechanisms show pure left-lateral strike-slip motion from the mid-Cayman spreading center to the southern Cuban margin [*Perrot et al.*, 1997] where the fault trace slightly changes direction to become transpressional [*Calais and de Lepinay*, 1991], with earthquake focal mechanisms showing a combination of thrust and strike-slip faulting [*Van Dusen and Doser*, 2000]. To the east, the Oriente fault pursues its course through the Windward Passage, along the northern Haitian coast as the "Septentrional fault" [*Calais and de Lépinay*, 1990], then farther east on land through the Cibao Valley of the Dominican Republic [*Calais and de Lépinay*, 1992] where paleoseimological studies indicate a Holocene slip rate of 9 $\pm$ 3 mm/yr [*Prentice et al.*, 2003], in agreement with GPS estimates [*Calais et al.*, 2002]. The Septentrional fault extends offshore to the east as far as the Mona rift, one of the active structures marking the extensional boundary between Hispaniola and Puerto Rico through the Mona Passage [*Grindlay et al.*, 1997; *Gestel et al.*, 1998]. The continuation of the Septentrional fault east of the Mona Passage is less clear (Figure 2), it may gradually merge with the Puerto Rico trench through a series of small faults including the Bunce and Bowin faults [*ten Brink et al.*, 2004; *Grindlay et al.*, 2005b]. The Septentrional fault was the locus of significant historical earthquakes, among which the destructive 1842, *M*8.0, Cap Haitian earthquake in Haiti and the 1562, *M*7.7, Santiago earthquake in the Dominican Republic [*Scherer*, 1912; *McCann*, 2006; *ten Brink et al.*, 2011].

The Cayman trough is bounded to the south by a second series of left-lateral strike-slip faults, starting at the mid-Cayman spreading center with the purely strike-slip Walton fault [*Rosencrantz and Mann*, 1991]. The Walton fault connects through Jamaica with the Enriquillo-Plantain Garden fault (EPGF) through a series of relays whose geometry remains debated [*Benford et al.*, 2012a]. The EPGF continues offshore as a purely strike-slip fault east of Jamaica then on land in southern Haiti where it is marked by a well-defined narrow valley continuing eastward just north of Port-au-Prince and into the Enriquillo Valley in the Dominican Republic [*Mann et al.*, 1995]. Farther east, the EPGF appears to merge with thrust faults at the western termination of the Muertos trough [*Mauffret and Leroy*, 1999]. A number of historical earthquakes, possibly located on that fault, struck southern Hispaniola between 1701 and 1770 [*Bakun et al.*, 2012]. The M_w7.1, 2010, Haiti earthquake ruptured one of the subsidiary faults of the EPGF system close to Port-au-Prince in a transpressional context [*Calais et al.*, 2010; *Hayes et al.*, 2010]. No geological estimate of slip rate is yet available for that fault.

The Muertos trough marks the front of a large accretionary prism that has developed along the southern margin of the Dominican Republic and Puerto Rico [*Byrne et al.*, 1985; *Granja Bruña et al.*, 2009]. It is associated with some seismicity, in particular a M_s6.7 thrust faulting event in 1984, that may mark the contact between a downgoing slab of Caribbean lithosphere under the Greater Antilles island arc [*McCann and Sykes*, 1984a]. Evidence for sediment deformation and active faulting becomes more tenuous eastward toward the Anegada Passage, a system of basins apparently bounded by active strike-slip and normal faults that separate Puerto Rico and the Virgin Islands from the Lesser Antilles to the south [*Masson and Scanlon*, 1991; *Jany et al.*, 1990]. The connection between the Anegada faults and the Puerto Rico/Lesser Antilles subduction is unclear, we will highly simplify its geometry in our model.

The northern margin of the Greater Antilles island arc marks the contact between the Caribbean plate and the obliquely subducting oceanic lithosphere of the North American plate. It is marked, in the west, by a narrow basin between the Bahamas carbonate platform and the island of Hispaniola, bounded along its southern edge by active compressional features revealed by side-scan sonar and seismic reflection data [*Dillon et al.*, 1996; *Dolan and Wald*, 1998] that define the North Hispaniola fault. Active shortening perpendicular to that fault is shown by the series of *M*7.2 – 8.1 thrust earthquakes that struck the northeastern Dominican Republic in 1943 – 1953 [*Dolan and Wald*, 1998] and by the more recent M_w6.4 thrust earthquake of 2003 offshore the northern Dominican Republic [*Dolan and Bowman*, 2004]. The North Hispaniola basin and fault are continuous to the east with the Puerto Rico trench, deepest point of the Atlantic Ocean (>8 km) and largest negative free-air gravity anomaly on Earth (−400 mGals), which marks the oblique subduction of the Atlantic oceanic lithosphere under Puerto Rico [*Sykes et al.*, 1982; *Calais et al.*, 1992; *Grindlay et al.*, 2005b].

To the east, the Puerto Rico trench curves around the Virgin islands but remains continuous with the Lesser Antilles trench further south. Contrary to Puerto Rico where plate motion is highly oblique to the trench direction, in the Lesser Antilles plate motion becomes perpendicular to the trench. A significant number of small to moderate earthquakes define the interface between the subducting slab and the overriding island arc along most of the Lesser Antilles subduction. Seismicity is, however, less prominent south of 15°N, coincident with the development of a thick accretionary prism fed by sediments shed from the South American continent [*Le Pichon et al.*, 1990]. North of that latitude, the arc is crosscut by a series of normal faults [*Feuillet et al.*, 2002], the Anegada fault zone possibly representing the northernmost of that extensional system.

At its southern termination, the lesser Antilles subduction bends around toward South America and connects with a mostly strike-slip plate boundary. GPS studies have shown that ~65% of the relative motion between the Caribbean and the South American plates was accommodated by strike-slip faulting on Trinidads' Central Range fault, a major structure connecting with the southern extent of the Lesser Antilles near Tobago and crossing the central part of Trinidad. Although it currently appears aseismic, paleoseismic investigations have shown that the Central Range fault in Trinidad produced several large earthquakes between 2710 and 550 years B.P. [*Prentice et al.*, 2010]. Additional motion most likely occurs on the Los Bajos fault of southern Trinidad and other offshore faults south of the island [*Weber et al.*, 2010; *Soto et al.*, 2007]. To the east, the main plate boundary fault continues offshore with a transtensional relay in the Gulf of Paria [*Babb and Mann*, 1999], then connects with the El Pilar-San Sebastian fault system which marks the Caribbean-South America in northern Venezuela [*Mann et al.*, 1990]. An unknown quantity of north-south shortening is taken up by compressional, accretionary prism-like structures offshore Venezuela and Colombia that form the "South Caribbean Deformed Belt" [*Kroehler et al.*, 2011].

The paleoearthquake record of the El Pilar fault is well established by trench excavations and historical records of destructive earthquakes [*Audemard et al.*, 2000; *Mendoza*, 2000]. Earthquake focal mechanisms and other kinematic indicators show pure right-lateral strike slip on vertical east-west trending planes [*Audemard et al.*, 2005]. GPS measurements across the El Pilar fault are consistent with these results and show that the El Pilar fault accommodates the totality of the Caribbean-South America strike-slip motion (20 to 22 mm/yr) [*Perez et al.*, 2011]. In addition, dense GPS measurements indicate up to 50% of aseismic slip on some segments of the El Pilar fault [*Jouanne et al.*, 2011]. The plate boundary broadens further west, with right-lateral motion taken up by the transpressional Bocono fault in western Venezuela and strike-slip motion on the Oca fault [*Dewey*, 1972; *Audemard et al.*, 2005]. The Bocono fault is a primarily right lateral strike-slip fault with a small component of compression [*Schubert*, 1982]. It merges with the El Pilar fault zone near Caracas and follows the Cordillera de Merida with a NE-SW trend. Early GPS measurements showed that the Bocono fault accommodates 9–11 mm/yr of dextral shear and ~1 mm/yr of compression [*Pérez et al.*, 2001]. The Bocono and Oca faults bound the triangular-shape Maracaibo block to the north and east, while its third boundary is marked by the less well-known Santa Marta-Bucaramanga fault system, where early GPS measurements indicate 6 ± 2 mm/yr of left-lateral slip [*Trenkamp et al.*, 2002].

2.2. Previous GPS-Based Models

Several attempts have been made to quantify the kinematics of plate boundary deformation in the Caribbean but only for specific plate boundary segments so far. Early on *Dixon et al.* [1998] used six GPS stations in the Dominican Republic to show eastward motion of the Caribbean plate with respect to North America at a rate twice faster than predicted by the Nuvel-1A geologic model [*DeMets et al.*, 1994], with slip accommodated on the Septentrional, Enriquillo, and North Hispaniola faults at rates that were then quite uncertain. The present-day kinematics of the Caribbean plate was later quantified in more detail by *DeMets et al.* [2000], who used four GPS stations in the plate interior to compute its first geodetically derived angular velocity. They confirmed that the Caribbean plate motion was significantly faster than predicted by Nuvel-1A, which was later shown to result from a global bias introduced by earthquake slip vectors at obliquely convergent plate margins [*DeMets and Dixon*, 1999]. Additional GPS measurements in the northeastern Caribbean allowed *Jansma et al.* [2000] to show the existence of a Puerto Rico-Virgin Islands block independent from the Caribbean plate, while *Calais et al.* [2002] provided the first estimates of strain accumulation rates on regional faults in Hispaniola and showed strain partitioning in an oblique collisional context. In the northern Lesser Antilles, *Lopez et al.* [2006] observed a systematic misfit between their GPS-derived Caribbean/North America relative plate motion and slip vectors of thrust earthquakes. They interpreted this observation—dependent on the definition chosen for the Caribbean frame—as indicative of a Northern Antilles block distinct from the Caribbean plate and moving with respect to it at rates up to 5 mm/yr. This would be consistent with the slip partitioning model proposed by *Feuillet et al.* [2002, 2010] on the basis of fault mapping and shallow focal mechanisms, which predicts 5 to 10 mm/yr of left-lateral shear along en échelon normal faults west of the islands and distributed trench parallel extension along the northern half of the Lesser Antilles.

The first regional-scale kinematic model for the Caribbean was proposed by *Manaker et al.* [2008] using a combined GPS solution covering Hispaniola and Puerto Rico, with a few sites in the northernmost part of the Lesser Antilles. They showed that the data were consistent with a simple block model with strain accumulation on the major plate boundary faults but with largely uncoupled Puerto Rico and Lesser Antilles subduction interfaces. They observed that the transition from a coupled to uncoupled plate interface coincided with the onset of oblique collision between the Greater Antilles island arc and the Bahamas platform [*Grindlay et al.*, 2005a]. The number of reliable GPS sites available in the Lesser Antilles was however small and the predicted strain accumulation highly uncertain, leading to a wide range of possible earthquake and tsunami scenario [*Hayes et al.*, 2014].

Manaker et al. [2008] results were updated locally following the 2010 Haiti earthquake [*Calais et al.*, 2010]. A surprising result then, thanks to a new GPS data set in Haiti, was evidence for shortening across Hispaniola, consistent with the transpressional nature of the 2010 Haiti event. *Benford et al.* [2012a] then used a dense campaign GPS network in Jamaica and argued for ~7 mm/yr of strike-slip motion across the island accommodated by the central Jamaican fault system on land (Rio Minho-Crawle River fault zone) and about 2 mm/yr of convergence offshore to the south of the island on unmapped faults on the northern Nicaragua rise. The combination of GPS velocities in Jamaica and Hispaniola allowed *Benford et al.* [2012b] to refine a regional kinematic model for the northern Caribbean by geodetically defining the boundary between the Gonave microplate [*Mann et al.*, 1995] and the Hispaniola block of *Manaker et al.* [2008] through western Hispaniola. They provided new estimates for the angular velocities of the Gonave, Hispaniola, north Hispaniola, and Puerto Rico microplates.

No kinematic model is yet available for the southern boundary of the Caribbean plate but several regional studies have already placed constraints on fault slip rates and locking depth, as noted above. *Pérez et al.* [2001] and *Weber et al.* [2001] showed that the Caribbean plate is currently moving due east with respect to South America at 20–22 mm/yr, with pure right-lateral strike slip concentrated in a narrow region along the El Pilar fault in Venezuela, possibly experiencing aseismic slip [*Jouanne et al.*, 2011]. In Colombia and northern Ecuador, GPS measurements show that plate boundary deformation involve the Maracaibo and North Andes blocks [*Trenkamp et al.*, 2002; *White et al.*, 2003]. The North Andes block is currently moving northward with respect to the Caribbean plate, consistent with recent evidence for large continental slivers along the south American margin from Peru to Ecuador [*Nocquet et al.*, 2014].

Though some is known—at least locally—on the first-order active tectonic features of the region, thanks to seismotectonic mapping, paleoseismology, and geodetic measurements, we are still lacking a geodetically consistent GPS velocity field covering the entire Caribbean plate and its boundaries. The complexity of plate boundary deformation in the region, the limited land areas, and the small number of GPS sites on the stable Caribbean plate require a large-scale approach in order to simultaneously estimate plate/block motions and plate boundary deformation in a kinematically consistent manner. The proximity of many GPS sites to active faults imposes that strain accumulation be accounted for, with the possibility of laterally variable coupling on subduction interfaces. In the following, we present a large-scale GPS velocity field covering the entire study, which we interpret in terms of rigid block motions and strain accumulation on locked or partially locked faults.

3. Data and Models

3.1. GPS Data Analysis

We processed data from 342 episodic and continuously recording GPS sites in the study area from 1994 onward using the GAMIT–GLOBK software package [*Herring et al.*, 2010a]. The data are usually openly available on public databases or upon request from private ftp sites. We process double-difference phase measurements to solve for station coordinates, satellite state vectors, seven daily tropospheric delay parameters per site, two parameters for horizontal tropospheric gradients, and phase ambiguities using final satellite orbits from the International Global Navigation Satellite Systems (GNSS) Service (IGS), Earth orientation parameters from the International Earth Rotation Service (IERS), applying corrections for solid Earth tides, polar tides, time-variable ocean loading following the IERS conventions 2010 [*Petit and Luzum*, 2010] and antenna phase-center variations using the latest IGS tables [*Schmid et al.*, 2007], and subsequent updates. For the later years when the number of stations increases significantly, we process the data in subnetworks of up to 40 sites, including 12 reference sites from the International GNSS Service (IGS) common to all subnetworks

(BDOS, BOGT, BRAZ, BRMU, CRO1, FORT, KOUR, MAS1, MDO1, NLIB, SCUB, WES2), and two additional common sites between subnetworks.

We identify discontinuities or offsets caused by changes in the instrumentation or to earthquakes by visually inspecting daily position time series. We account for these discontinuities in the velocity solution by allowing for a three-component offset while equating velocities before and after the offset. We remove some sections of time series with nonlinear deviation from the background trend due to postseismic deformation. This is, for instance, the case of 2009, *M*7.3, Swan Islands earthquake [*Graham et al.*, 2012], which caused significant coseismic and postseismic displacements at several GPS sites used here.

After this cleaning step, we combine the regional loosely constrained daily solutions with global daily solutions for the whole IGS network available from the Massachusetts Institute of Technology IGS Data Analysis Center into weekly position solutions. This helps improve signal resolution over the noise level and allows us to optimally tie our solution to the International Terrestrial Reference Frame (ITRF) [*Altamimi et al.*, 2011]. We finally combine these weekly solutions into a single position/velocity solution using GLOBK [*Herring et al.*, 2010b], which we tie to the ITRF by minimizing position and velocity deviations from a set of globally defined IGS reference sites common to our solution via a 12 parameter Helmert transform (scale and scale change are not estimated). We downweight the variance of the height coordinates by a factor of 10 because of the reduced precision of the vertical component in standard GPS solutions. We estimate time-correlated noise at continuous sites using the First-Order Gauss-Markov Extrapolation algorithm of *Herring*, [2003, see also *Reilinger et al.*, 2006a] in order to obtain realistic velocity uncertainties. For episodic sites, we include a 2 mm/$\sqrt{\text{yr}}$ random walk component to account for colored noise in velocity uncertainties.

The resulting solution is a set of coordinates and velocities expressed in ITRF2008, which can then be used to model the regional kinematics. Velocity uncertainties vary as a function of observation time span and reach 0.5 mm/yr for the oldest stations that have close to 20 years of continuous data (e.g., CRO1, BRMU, BOGT, and SCUB). A number of important observations are readily apparent on the velocity field shown in Figure 2 with respect to the North American (top) and Caribbean (bottom) plates. The Caribbean plate moves in an ENE direction with respect to North America at about 19 mm/yr, while North and South America are converging toward each other at a very slow rate (<2 mm/yr) increasing from east to west. This implies frontal convergence along most of the Lesser Antilles arc, transitioning to oblique subduction to the north in the Greater Antilles and pure strike slip along the boundary with South America.

In a Caribbean frame, GPS sites on the Nicaragua Rise, the Venezuelan basin, and the Lesser Antilles show velocities that are within error of zero, with a weighted RMS of residuals of 0.5 mm/yr and a maximum residual velocity of 1.5 mm/yr. We also find velocities close to zero at GPS sites in Puerto Rico and the Virgin Islands, except for the recently installed CN03 site in Virgin Gorda, with however a slight but systematic pattern of counterclockwise rotation. We observe about 3 mm/yr of extension across the Mona Passage, consistent with findings from earlier GPS measurements [*Jansma et al.*, 2000] and evidence for extensional faulting between Puerto Rico and Hispaniola [*Gestel et al.*, 1998]. West of the Mona Passage in Hispaniola velocities show a N-S gradient consistent with strain accumulation on ~E-W directed, strike-slip plate boundary faults. The velocity difference is about 10 mm/yr across the Septentrional fault in the northern Dominican Republic and 6 mm/yr across the Enriquillo fault in southern Haiti. We also observe a N-S gradient in velocities across the central and western parts of Hispaniola with up to 4 mm/yr of shortening. The velocity gradient across Jamaica is consistent with strain accumulation on east-west directed faults across the island [*Benford et al.*, 2012b]. Along the southern boundary of the Caribbean plate, most of the Caribbean-South America relative motion is taken up by the El Pilar fault, then by the Bocono fault system farther to the west, while the Oca fault appears to accommodate slow relative motion between the Maracaibo block and the Caribbean plate.

3.2. Model Setup

We now model the observed GPS velocities by assuming that they represent the sum of rigid block rotations and strain accumulation on faults locked to a given depth in an elastic half-space. This approach, commonly called "kinematic block modeling," is widely used to analyze regional GPS velocity fields and quantify plate motions and slip deficit on locked or partially locked active faults [e.g., *McCaffrey*, 2002; *Meade et al.*, 2002; *Reilinger et al.*, 2006b; *Saria et al.*, 2014]. Here we use the modeling approach and associated code "blocks" described in *Meade and Loveless* [2009] where active faults are treated as freely slipping at the full relative plate motion below a given seismogenic depth above which there are either locked or partially slipping. In both cases the fault elastic contributions are calculated using the classical back-slip approach [*Savage*, 1983]

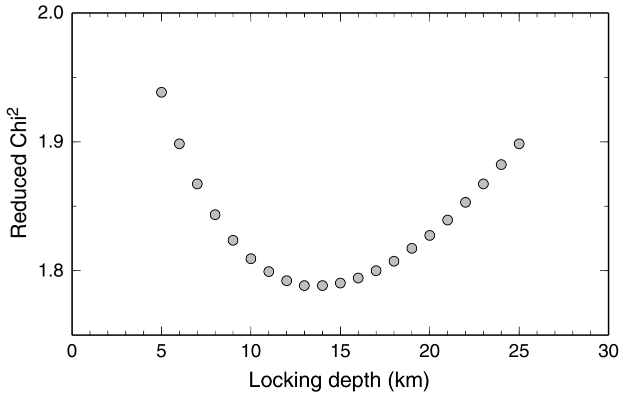

Figure 3. Model reduced χ^2 as a function of fault locking depth illustrating the minimum found for 14 km.

with Okada Green's functions in an elastic half-space [*Okada*, 1985]. Partially locked faults (in this case the subduction interface) are discretized using triangular elements. Continuity between fault elements and regularization of the solution are ensured by imposing a smoothing constraint that minimizes the Laplacian of the slip estimated along the fault plane. This method leads to a set of linear equations which allow for a well-defined solution. It also allows the plate interface to slip not only in the direction of the rigid differential block motion but also in the opposite direction to account for coseismic slip that could be associated with documented earthquakes, slow slip events, or postseismic deformation. A coupling coefficient can be calculated a posteriori by dividing the full relative plate motion by the estimated slip rate on each fault element.

Here we use the major known active faults as plate and block boundaries, following previous authors [*Manaker et al.*, 2008; *Benford et al.*, 2012b, 2012a]. We treat all faults as locked to a given depth, except for the Hispaniola-Puerto Rico-Lesser Antilles subduction which we discretize with triangular elements on which we solve for slip. We determined the optimal fault locking depth by running a series of models with locking depth ranging from 5 to 25 km. We find the lowest χ^2 for a locking depth of 14 km (Figure 3), which we then impose in all model runs. This locking depth is consistent with the seismogenic depth on intra-arc faults along the Caribbean margin and other similar tectonic settings [*Sanchez-Rojas and Palma*, 2014; *Miller et al.*, 2009]. We did not allow for the shallower locking depths proposed for the El Pilar fault [*Jouanne et al.*, 2011; *Weber et al.*, 2010] because our data set does not include sufficiently dense measurements in these regions to be sensitive to aseismic slip.

We derive the geometry of the subduction interface using its surface trace along the Lesser Antilles, Puerto Rico, and North Hispaniola trenches and the depth distribution of thrust earthquakes derived from the *Engdahl et al.* [1998] database (Figure 4). We limit the downdip end of the partially locked subduction interface using theoretical isotherms of fore-arc thermal structure between Guadeloupe and Barbados [*Gutscher et al.*, 2010; *Manga et al.*, 2012] which place the 350°C isotherm, considered as the downdip limit of purely seismogenic behavior, at a depth of about 40 km [*Hyndman*, 2007]. We find that shallow seismicity generally defines a plate interface of fairly constant and low-angle dip down to 40–60 km, below which the dip angle increases as the subducting slab bends [*Laigle et al.*, 2013], as apparent in Figure 4. We therefore use a single dip angle for each subduction segment. From the depth distribution of thrust earthquakes, we determine a plate interface dip of 20° north of Hispaniola, 25° along the Puerto Rico trench, and 16° for the Lesser Antilles. This latter value is consistent with seismic refraction data [*Kopp et al.*, 2011; *Laigle et al.*, 2013] at close distance to the trench. Therefore, we model the subduction as a curved fault with 20 segments of constant dip and a constant locking depth of 40 km (Figure 4). Assuming a Moho depth of 25–30 km under the Lesser Antilles as imaged by *Kopp et al.* [2011] between Guadeloupe and Dominica, the 40 km downdip end of the plate interface in the models is located just below the tip of the mantle wedge and allows for "deep flat-thrust" earthquakes as identified by *Laigle et al.* [2013].

3.3. Model Results

Our objective is to determine the best fit angular velocity for rigid block motions along the boundaries of the Caribbean plate to estimate the rate of interseismic strain accumulation on the major plate boundary faults. To do so, we ran a series of models with various block geometries starting with a single Caribbean plate and progressively complexifying the model geometry by fragmenting the plate boundaries into blocks (Figure 5). We assess the improvement obtained by increasing the model complexity (more blocks, i.e., increased degree of freedom) by testing the significance of the decrease in χ^2 from a model

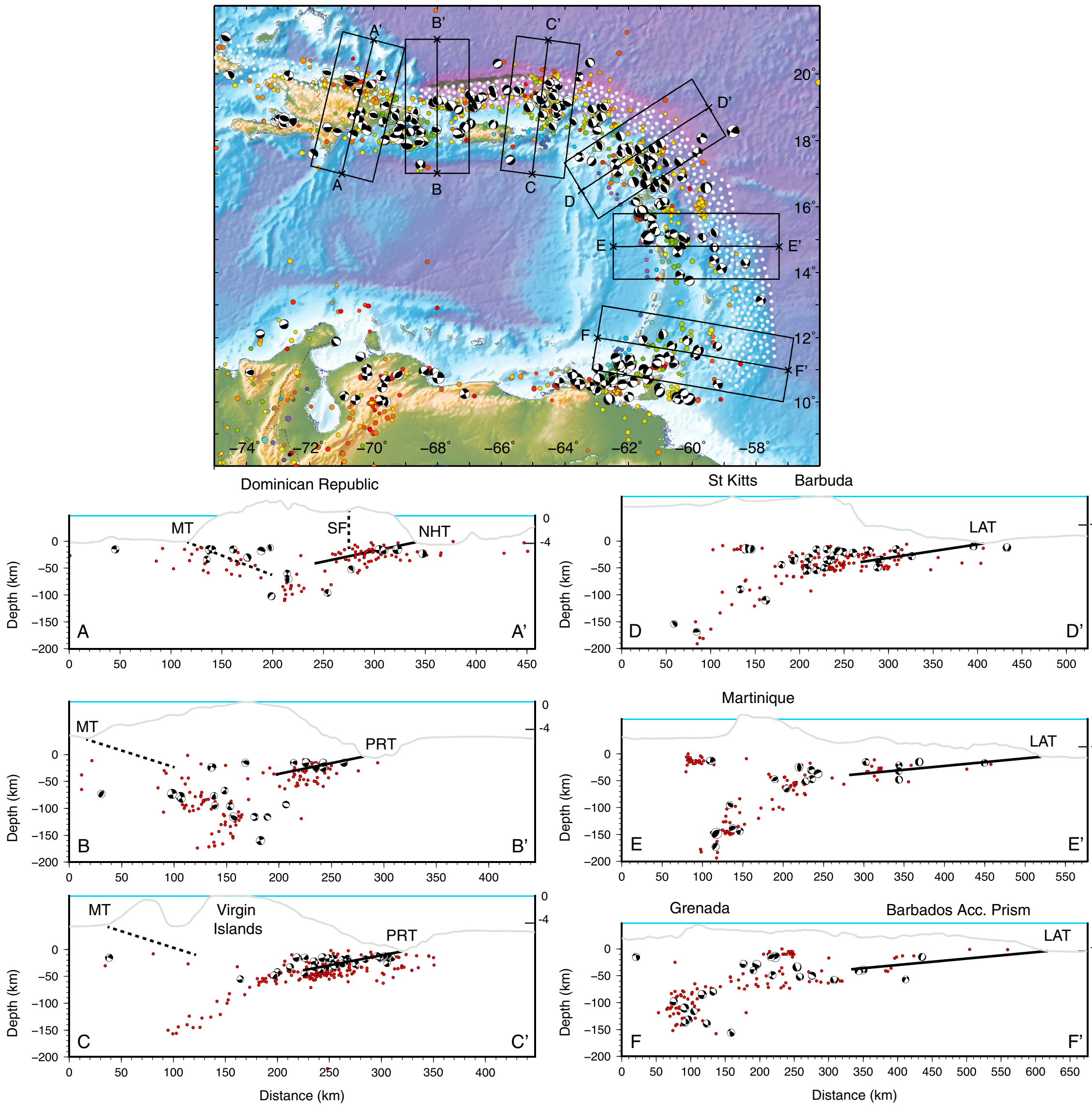

Figure 4. Earthquake focal mechanisms [*Ekstrom et al.*, 2012] and locations [*Engdahl et al.*, 1998] along the subduction interface and cross sections showing with a thick black line the position of the Caribbean-North America plate interface used in the model. Other faults are shown with thick dashed black lines. SF = Septentrional fault, PRT = Puerto Rico trench, MT = Muertos trench, LAT = Lesser Antilles trench, NHT = Northern Hispaniola trench. White dots on the map (top) show the vertices of the triangles used to discretize the subduction interface. Grey lines on cross section show the bathymetry with significant vertical exaggeration compared to the earthquake depth scale. The area used for each cross section is shown by a black rectangle on the top map.

with fewer blocks to a model with more blocks using the F ratio statistics (e.g., Stein and Gordon, 1984) given by

$$F = \frac{\left(\chi^2_{p_1} - \chi^2_{p_2}\right)/(p_1 - p_2)}{\chi^2_{p_2}/p_2} \tag{1}$$

where $\chi^2_{p_1}$ and $\chi^2_{p_2}$ are the chi-square statistics of two models with p_1 and p_2 degrees of freedom, respectively. We compare this experimental F ratio to the expected value of a $F(p_1 - p_2, p_1)$ distribution for a given risk level α% (or a $100 - \alpha$% confidence level) that the null hypothesis (the decrease in χ^2 is not significant) can be rejected. We set the acceptable significance level to 99%, i.e., a probability of rejection less than 1%. Figure 6 shows the variation in χ^2 and its significance level from one model to the next (see also Table 1).

Model 1, with a single unfragmented Caribbean plate, naturally results in the largest χ^2 (Table 1) and residuals, in particular in Colombia, Hispaniola, and Puerto Rico. Model 2 adds the northern Caribbean blocks defined by

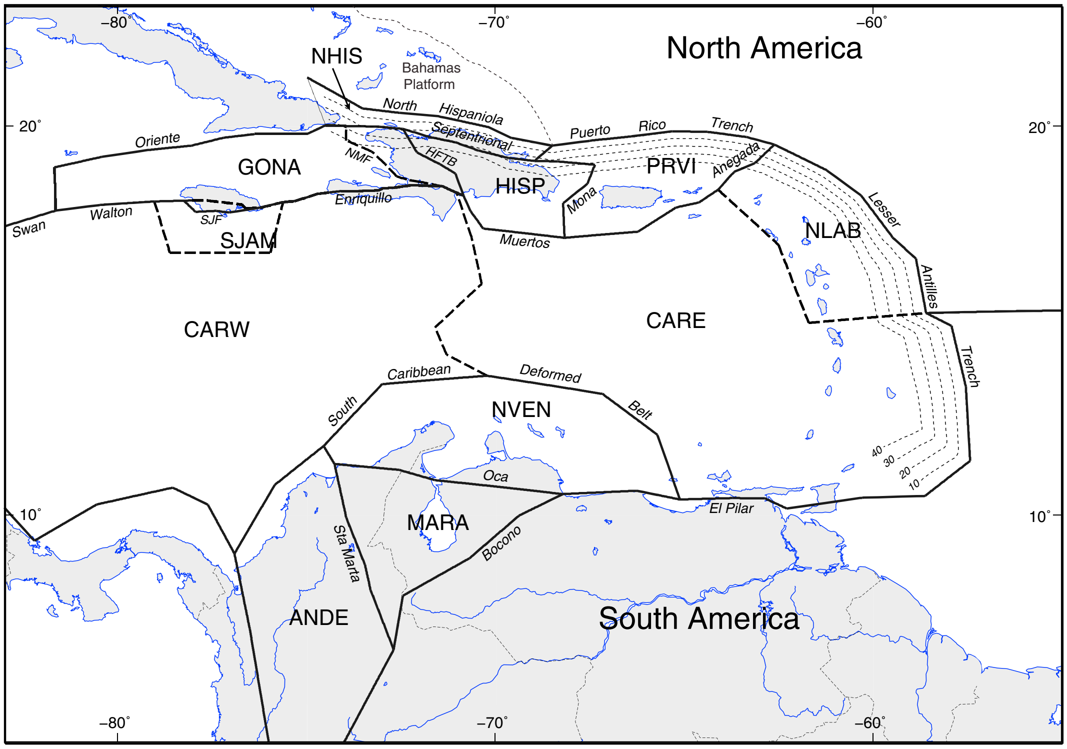

Figure 5. Block geometry used in the models tested. Solid black lines show the block boundaries for the best fit model, thick dashed lines show other tested block boundaries. NHIS = North Hispaniola, PRVI = Puerto Rico and Virgin Islands, GONA = Gonave, HISP = Hispaniola, NLAB = North Lesser Antilles Block, SJAM = South Jamaica. CARW = Caribbean West, CARE = Caribbean East, NVEN = North Venezuela, MARA = Maracaibo, ANDE = Andes, HFBT = Hispaniola fault and thrust belt, NMF = Neiba-Matheux thrust, SJF = South Jamaica fault. Thin dashed lines are depth contours of the subduction interface used in the model, derived from the earthquake hypocenters cross sections shown in Figure 4.

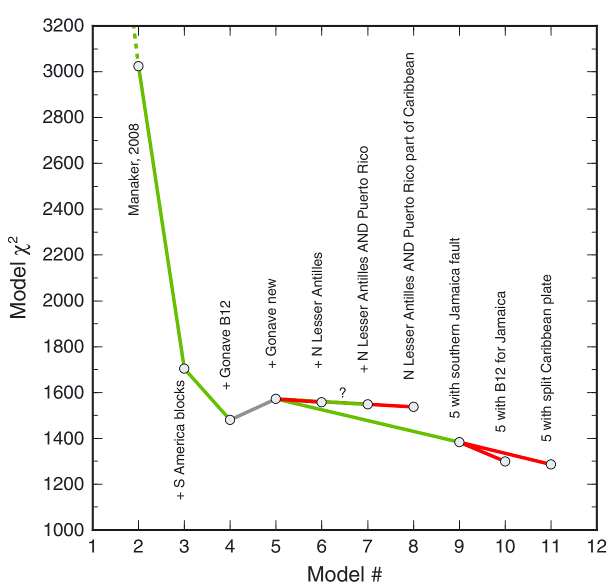

Figure 6. Total model χ^2 as a function of model tested. The line joining two models is green if the null hypothesis that the two models are similar can be rejected at a confidence level greater than 99%. It is red otherwise.

Manaker et al. [2008]. As expected, the improvement is significant well above the 99% confidence level, with much smaller residuals in Puerto Rico and Hispaniola, though still significant ones (3–4 mm/yr) in Jamaica. Model 3 further fragments the southern margin of the Caribbean plate with three blocks, Maracaibo, North Andes, and North Venezuela (Figure 5). The improvement is again significant at the 99% confidence level, as expected given the known regional tectonics, with residual velocities for these blocks less than 1.5 mm/yr.

Model 4 splits the Hispaniola block into two microplates, with a Gonave microplate extending from the mid-Cayman spreading center to the Neiba-Matheux thrust front (NMF in Figure 5) across central Hispaniola following *Benford et al.* [2012b]. Velocity residuals decrease significantly in northern Jamaica and Hispaniola, in

Table 1. χ^2 Variations Among Tested Model and Associated *F* Ratio Test Results[a]

Model A	Model B	DOF-A	DOF-B	$\Delta(\chi^2)$	F_{ratio}	*P* (%)
Model 1	Model 2	588	579	1976.145	47.023	0.01
Model 2	Model 3	579	570	1320.590	60.476	0.01
Model 3	Model 4	570	567	222.050	36.149	0.01
Model 4	Model 5	567	567	−91.539	-	-
Model 5	Model 6	567	564	15.424	2.5313	5.67
Model 5	Model 7	567	567	9.608	-	-
Model 8	Model 5	570	567	10.128	1.6488	17.7
Model 5	Model 9	567	567	153.782	-	-
Model 9	Model 10	567	564	85.456	17.430	0.01
Model 9	Model 11	567	564	11.796	2.228	8.39

[a]See also Figure 6. DOF = degrees of freedom, *P* = probability of rejection of the null hypothesis.

particular in the northern part of Haiti where they reach 2–3 mm/yr. However, this model predicts a large (up to 10 mm/yr) slip rate on the Neiba-Matheux faults, inconsistent with the lack of significant historical earthquakes on this structure and the subdued geomorphic expression of active deformation compared to the Enriquillo and Septentrional faults [*Mann et al.*, 1995; *Pubellier et al.*, 2000]. As shown by *Benford et al.* [2012b] with a sparser GPS data set, the location of the eastern boundary of the Gonave microplate is uncertain and could also be a broad zone of deformation across Hispaniola. We tested several locations for that boundary and obtained the lowest reduced χ^2 (2.047) for a trace that is coincidental with the Plateau Central-San Juan Valley area across Haiti and the Dominican Republic (perhaps the Peralta-Rio Ocoa belt of *Heubeck et al.* [1991]). In this configuration (model 5), residual velocities are < 1 mm/yr for all GPS sites in Hispaniola. This location of the block boundary, with predicted slip rates < 4 mm/yr, is consistent with historical events in 1761, which caused severe damage in the Neiba-San Juan area, and 1911 (*M*6.9?), which destroyed the cathedral of San Juan and was strongly felt in Hinche and Grande Rivière in Haiti [*Scherer*, 1912].

We then test a scenario (model 6) that further splits the northeastern Caribbean plate margin with an additional North Lesser Antilles block, following [*Lopez et al.*, 2006]. We bound the block to the north by the Anegada passage fault and to the west by the strike-slip back-arc fault system described by [*Feuillet et al.*, 2002]. We set its southern boundary to the latitude of Dominica which coincides with the intersection of the Lesser Antilles subduction with the North America-South America plate boundary [*Pichot et al.*, 2012]. The reduced χ^2 improves slightly but with a confidence level less than 99% compared to a model that does not include that block (model 5, Table 1). Residual velocities are essentially unchanged compared to model 5. They are within observation errors for all GPS sites in the Lesser Antilles and do not show any systematic pattern. This therefore indicates that the existence of a North Lesser Antilles block separate from the Caribbean plate is not required by the GPS data.

We further test this result by computing a series of angular velocities for the Caribbean plate starting with the four sites used by *DeMets et al.* [2000] (SANA, ROJO, CRO1, and AVES), then adding one by one the best-determined GPS sites in the Lesser Antilles (velocity uncertainty <2.5 mm/yr). We use the *F* test described above to determine whether the null hypothesis—a model with or without a given site is similar—can be confidently rejected. We choose a conservative 99% confidence here. If the null hypothesis can be confidently rejected, then the site velocity is not consistent with the rigid plate rotation. We find that the null hypothesis can be confidently rejected for only three of the 42 reliable GPS sites in the Lesser Antilles (Figure 7). Two of them (sites SOUX and PSA1), less than a kilometer from each other, are located near the top of the Soufrière volcano of Guadeloupe in an area affected by nontectonic deformation related to local hydrothermal processes and slope instabilities. The third one, site MPCH, was measured in survey mode only and has a short and discontinuous time series. We conclude that the GPS data are therefore consistent with a Lesser Antilles arc that moves coherently with the rest of the Caribbean plate, at the uncertainty level of the GPS errors (0.6 mm/yr Weighted Root Mean Square (WRMS)).

Model 5 predicts <1.2 mm/yr motion on the Anegada Passage fault system (Virgin Island basin, Anegada Passage *s.s*, and Sombrero basin) [*Jany et al.*, 1990] and only up to 1.5 mm/yr of shortening across the eastern Muertos trough south of Puerto Rico. We therefore tested a model that merges the Puerto Rico and North

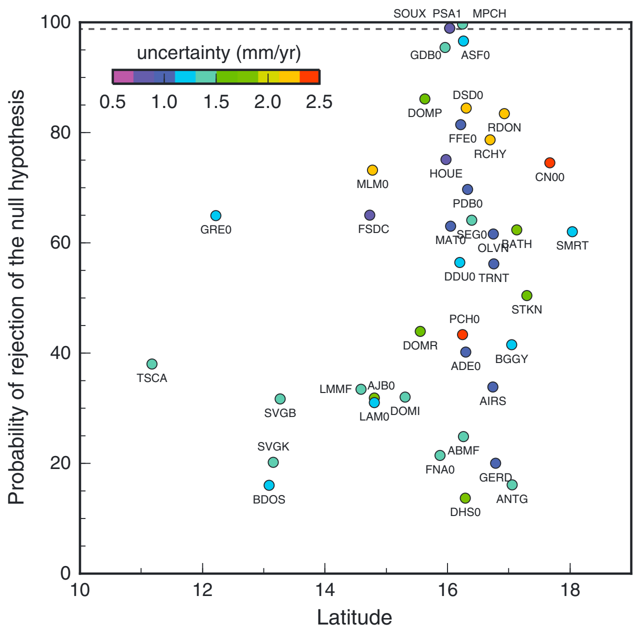

Figure 7. Test of the consistency of Lesser Antilles GPS velocities with the rigid rotation of the Caribbean plate. The *y* axis shows the probability that the null hypothesis — a model with or without a given site is similar — can be rejected. We find that only three sites (SOUX, PSA1, and MPCH) can be confidently rejected as not consistent with a rigid Caribbean plate motion. Colors show the site velocity uncertainties.

Lesser Antilles blocks into a single microplate distinct from the Caribbean plate (model 7). We find a similar reduced χ^2 as in model 5, with insignificant slip (<0.1 mm/yr) on the Caribbean-Northern Lesser Antilles boundary, consistent with the lack of relative motion resolvable by the data between the Lesser Antilles and the Caribbean plate. We further test a model where the Puerto Rico and the North Lesser Antilles blocks are both part of the Caribbean plate (model 8). We find that the decrease in χ^2 from that model to one where the Puerto Rico block is separate from the Caribbean plate (model 5) is significant at 82% confidence level only.

We therefore conclude that the GPS data do not require a North Lesser Antilles block and are only marginally able to distinguish a Puerto Rico block separate from the Caribbean plate. This is already visible in Figure 2 and consistent with the very low slip rates predicted by model 5 along the eastern Muertos and Anegada Passage faults, close the GPS velocity uncertainties. However, because model 5 is still statistically superior and because active deformation is documented — though at an unknown rate — on the eastern Muertos and Anegada Passage faults, we will keep it as our best fit model thus far.

We then turn our attention to Jamaica, starting with model 5 which includes a single fault through central Jamaica, shows residuals within measurement errors north of that fault but large westward residuals south of it. Residual velocities at continuous GPS sites CN10 and CN11 (or their corresponding campaign sites MCAY and PEDR) offshore Jamaica on the Nicaragua Rise are, however, close to zero, consistent with the Caribbean plate motion. This indicates that the active fault responsible for residual velocities in southern Jamaica must lie somewhere between these sites and the island. We therefore replaced the central Jamaica fault by a southern Jamaica fault following the South Coastal and Aeolus Valley faults also tested by *Benford et al.* [2012b] as the boundary between the Gonave microplate and the Caribbean plate (model 9). This results in a much improved fit across Jamaica while residual velocities at sites CN10 and CN11 remain consistent with the Caribbean plate. We also tested the preferred block configuration of *Benford et al.* [2012b] (model 10) with a Nicaragua Rise block carrying sites CN10/CN11 (MCAY/PEDR) and bounded to the north by a central Jamaica fault. This model predicts small slip rates (< 1 mm/yr) on the central Jamaica fault and significant ones (up to 6 mm/yr) along the west, east, and south boundaries of that block. This is difficult to justify in the absence of significant offshore geological features capable of accommodating this large amount of displacement. The best fit model, therefore, emphasizes fault activity in the southern part of the island, consistent with the location of the largest historical earthquakes to strike Jamaica in 1692 and 1907 [*Wiggins-Grandison*, 2004]. However, given the uncertainties in the GPS velocities, this result does not preclude the existence of other seismogenic faults through and around Jamaica accommodating part of the Gonave/Caribbean relative motion.

Finally, we evaluate with model 11 whether the data require splitting the Caribbean plate into two subplates, for instance, along the eastern edge of the Beata Ridge as proposed by *Leroy and Mauffret* [1996]. We obtain a fit very similar to model 9. An *F* test shows that the null hypothesis that a two-plate model versus one-plate model are similar cannot be rejected at a significance level greater than 99%. We conclude that the current regional data set does not require splitting the Caribbean plate. Longer observational time series at continuous sites on the Nicaragua Rise, in particular, will be essential to confirm or refine this statement.

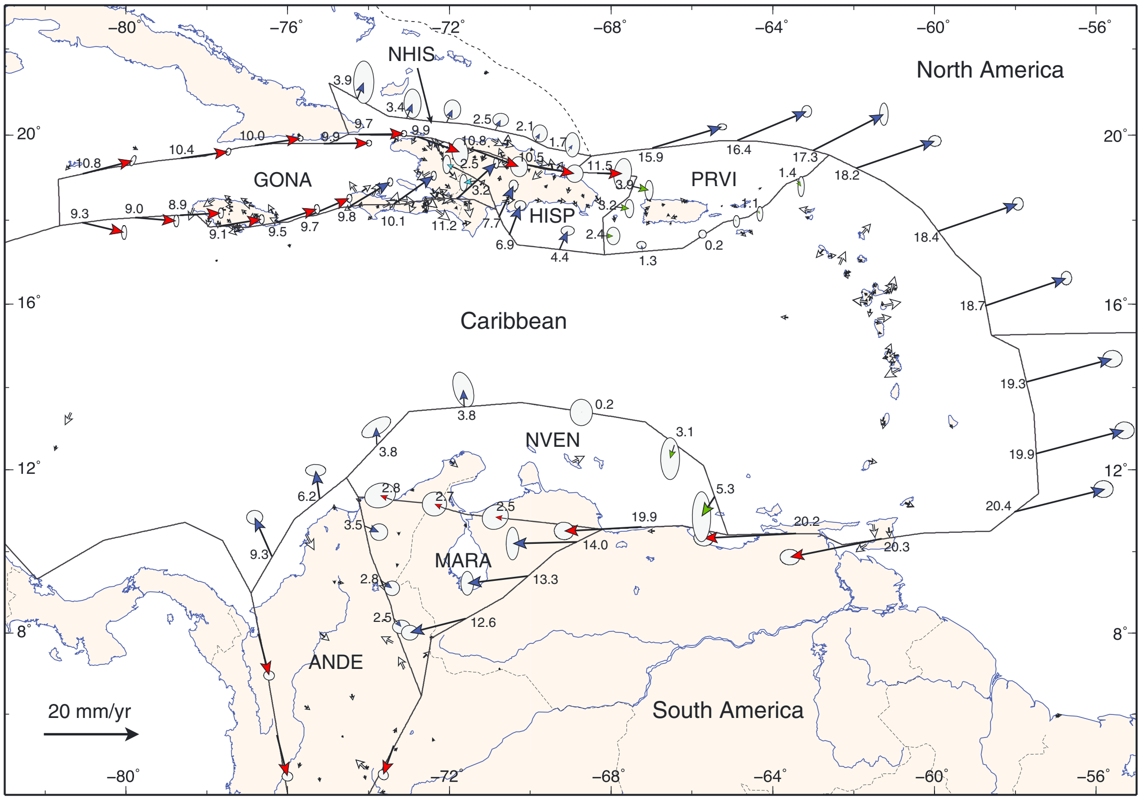

Figure 8. Best fit model geometry with block boundaries as solid black lines and predicted relative block motions as arrows with velocity indicated in mm/yr with their 95% confidence ellipse according to the parameters listed in Table 2. Red = strike slip (i.e., slip direction with $\pm 30^{o}$ from fault strike), blue = reverse or transpressional, green = normal of transtensional. Residual velocities are shown with grey arrows. We omitted their error ellipses for a sake of readability, see Figures 9 and 10 for a close up view on Hispaniola and the Lesser Antilles. The thin dashed line indicates the boundary of the Bahamas Platform.

4. Discussion

4.1. Best Fit Model

In the end, Figure 8 provides the best fit to the GPS data used here with the simplest block geometry required by the data. Velocity residuals are within measurement uncertainties at all sites and are randomly distributed, without systematic pattern (Figures 9 and 10). Estimated plate and block angular velocities (Table 2 and Figure 11) are well determined, thanks to the significant number of GPS sites available, except for the North Hispaniola block whose angular velocity estimate relies on a small number of sites over a small geographic footprint. Contrary to *Manaker et al.* [2008], we did not constrain the angular rotation of the Caribbean plate to the *DeMets et al.* [2000] value but estimated it. Our Caribbean-North America angular velocity agrees with the most recent global 3.2 Ma geological estimate [*DeMets et al.*, 2000] within errors. It is close to, but significantly different from the *Benford et al.* [2012a] or the older *DeMets et al.* [2000] estimates (Figure 11). We also find a Puerto Rico-North America angular velocity similar to that of *Benford et al.* [2012a].

In the northern Caribbean, the best fit model predicts pure strike-slip motion along the EPGFZ (~9 mm/yr), Septentrional (~10 mm/yr), and Oriente (~10 mm/yr) faults (Figure 8). These results are consistent with previous estimates [e.g., *Manaker et al.*, 2008; *Calais et al.*, 2010]. In addition, the model predicts significant shortening along the Enriquillo fault system through southern Haiti, with 5 to 7 mm/yr (west to east) of plate boundary-perpendicular motion. This is similar to—though slightly larger than—the results of the latest kinematic block model for the northern Caribbean by *Benford et al.* [2012a]. This new finding likely results from the significant improvement in GPS site distribution in Haiti and is consistent with the transpressional nature of the 2010 Haiti earthquake whose moment release was two thirds strike slip and one third reverse motion [*Calais et al.*, 2010].

The best fit model predicts slow N-S convergence (2 to 4 mm/yr from east to west) across the North Hispaniola fault, consistent with the source mechanisms of the 1946 [*Dolan and Wald*, 1998] and 2003 [*Dolan and Bowman*, 2004] earthquakes off the northern coast of the Dominican Republic. A similar conclusion was

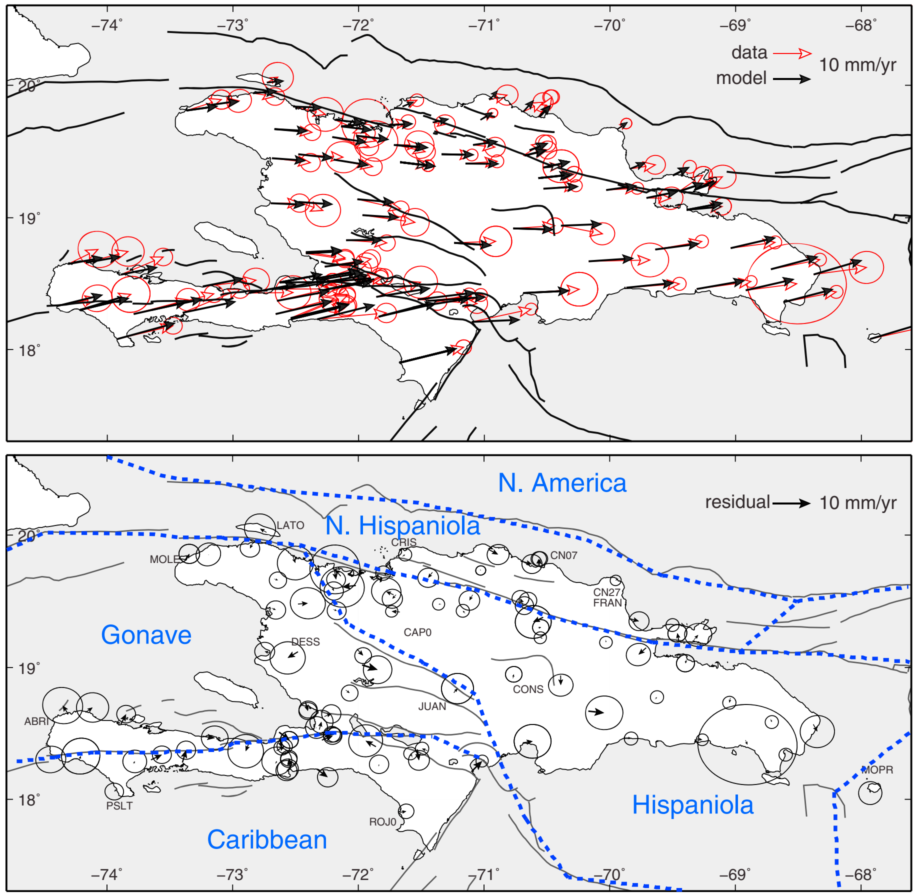

Figure 9. (top) Observed and modeled velocities in Hispaniola shown with respect to the North American plate. (bottom) Residual velocities. Dashed blue lines show the block boundaries, with block names labeled in blue. Error ellipses are 95% confidence.

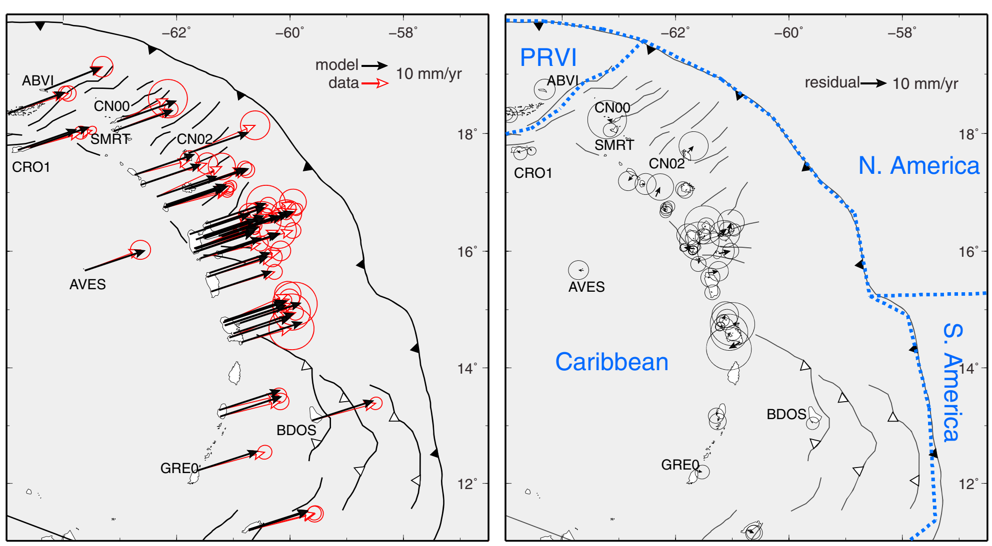

Figure 10. (left) Observed and modeled velocities in the Lesser Antilles shown with respect to the North American plate. (right) Residual velocities. Dashed blue lines show the block boundaries, with block names labeled in blue. Error ellipses are 95% confidence.

Table 2. Angular Velocity Estimates With Respect to the North American Plate for the Best Fit Model Described in the Text and Previously Reported Values[a]

Block/Plate	Angular Velocity Latitude (°N)	Longitude (°E)	ω (°/Myr)	Rotation Uncert. (°/Myr)	Error Ellipse Smaj (deg)	Smin (deg)	Azim (deg)	Rotation Vector Ω_x	Ω_y (°/Myr)	Ω_z	Covariance Elements C_{xx}	C_{xy}	C_{xz} (10^{-10} radian^2/Myr^2)	C_{yy}	C_{yz}	C_{zz}
This Work																
Caribbean	−71.60	47.77	0.179	0.004	8.0	0.8	15.2	0.0380	0.0418	−0.1698	71	−136	44	276	−88	32
South America	16.61	−53.58	0.136	0.006	2.6	1.7	83.8	0.0774	−0.1049	0.0389	42	−50	−1	83	1	10
Puerto Rico	−34.76	107.47	0.518	0.138	11.6	0.6	70.6	−0.1278	0.4059	−0.2954	9085	−20935	7575	48338	−17482	6336
Maracaibo	0.24	−65.42	0.635	0.180	8.4	1.0	126.7	0.2642	−0.5774	0.0026	8971	−28470	5132	90980	−16387	3013
Andes	2.40	−69.31	1.003	0.054	0.9	0.3	141.4	0.3541	−0.9375	0.0420	657	−2321	268	8352	−962	126
North Venezuela	−0.26	−64.37	0.687	0.194	9.7	1.5	118.0	0.2972	−0.6194	−0.0032	12712	−36097	7945	104016	−22854	5176
Gonave	10.24	−74.11	0.533	0.047	1.9	0.5	103.2	0.1436	−0.5045	0.0948	373	−1452	495	5866	−1994	688
North Hispaniola	17.37	−65.73	0.234	0.282	15.9	3.5	154.7	0.0918	−0.2036	0.0698	23501	−67220	25268	193030	−72514	27361
Dominican Republic	−24.34	109.98	1.115	0.168	2.1	0.4	87.6	−0.3471	0.9548	−0.4595	9265	−25135	9081	68419	−24730	8957
Benford et al. [2012]																
Caribbean	−73.80	21.00	0.192	0.004	9.6	2.1	4.2	0.0500	0.0192	−0.1844	48	−108	30	513	−125	50
Puerto Rico	34.00	−73.20	0.605	0.135	9.4	0.7	112.5	0.1450	−0.4802	0.3383	8642	−19831	7143	45684	−16448	5935
Gonave	−4.10	106.50	0.473	0.065	5.0	1.1	80.4	−0.1340	0.4524	−0.0338	769	−2880	987	11494	−3934	1358
DeMets et al. [2010] (MORVEL)																
Caribbean	73.90	−147.40	0.190	0.005	8.2	1.5	169.6	−0.0444	−0.0284	0.1825	46	−109	29	356	-94	56
DeMets et al. [2000]																
Caribbean	64.9	250.5	0.214	0.030	29.2	3.0	−35.0	−0.0303	−0.0647	−0.2017	–	–	–	–	–	–

[a] smaj, smin, and azim are, respectively, the semimajor axis length, semiminor axis length, and azimuth of the semimajor axis clockwise from north for the 95% confidence ellipse associated with the angular velocity estimate.

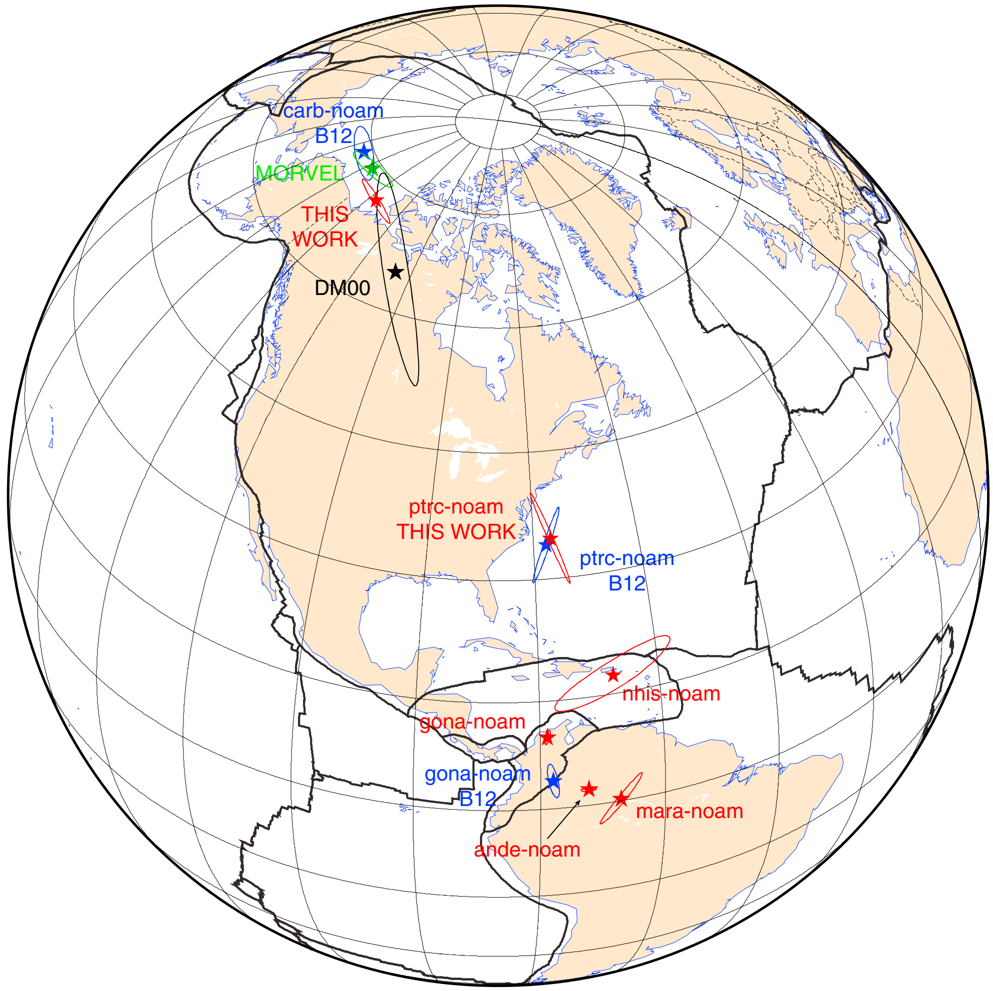

Figure 11. Euler poles for block pairs with their 95% confidence ellipse. The four stars in northernmost part of the figure show the Caribbean-North America Euler pole for this work in red, *DeMets et al.* [2000] in black, *Benford et al.* [2012a] in blue, and *DeMets et al.* [2010] in green. Note the general agreement between this work and *Benford et al.* [2012a], although the two 95% confidence error ellipses do not overlap. The same holds for the Gonave-North America relative motion. The agreement between the two studies is, however, excellent for the Puerto Rico-North America angular velocity estimate.

reached by *Manaker et al.* [2008], who however imposed earthquake slip vector directions as a constrain in the kinematic inversion. This result confirms the partitioning of the highly oblique convergence between the Caribbean and North America plate between intra-arc strike-slip faults and convergence at the plate interface [*Calais et al.*, 2002]. The model also predicts a moderate amount of convergence (~1–3 mm/yr) across central Hispaniola along the boundary between the Gonave and Hispaniola microplate, possibly coincident with the Hinche-San Juan valley fault zone [*Pubellier et al.*, 2000] or distributed over a broader region. This result should prompt additional geological work to try to identify paleoearthquakes in this supposedly aseismic region. Finally, the model indicates significant oblique shortening across the western part of the Muertos trough (~5–6 mm/yr), consistent with active compressional structures well imaged by offshore seismic reflection data [*Ladd et al.*, 1977; *Granja Bruña et al.*, 2014].

We find no evidence for internal deformation of the Puerto Rico-Virgin Island block at the ~0.5 mm/yr level (RMS of residual velocities), consistent with the absence of significant active faulting [*Frankel et al.*, 1980]. Holocene faulting within Puerto Rico reported, in particular, on the Cerro Goden-Great Southern fault zone [*Grindlay et al.*, 2005a] therefore has to be occurring on very slow slipping faults. The Caribbean-North America plate motion along that segment of the plate boundary is accommodated by oblique slip on the plate interface, consistent with slip vector directions of instrumental earthquakes (Figure 1), though a

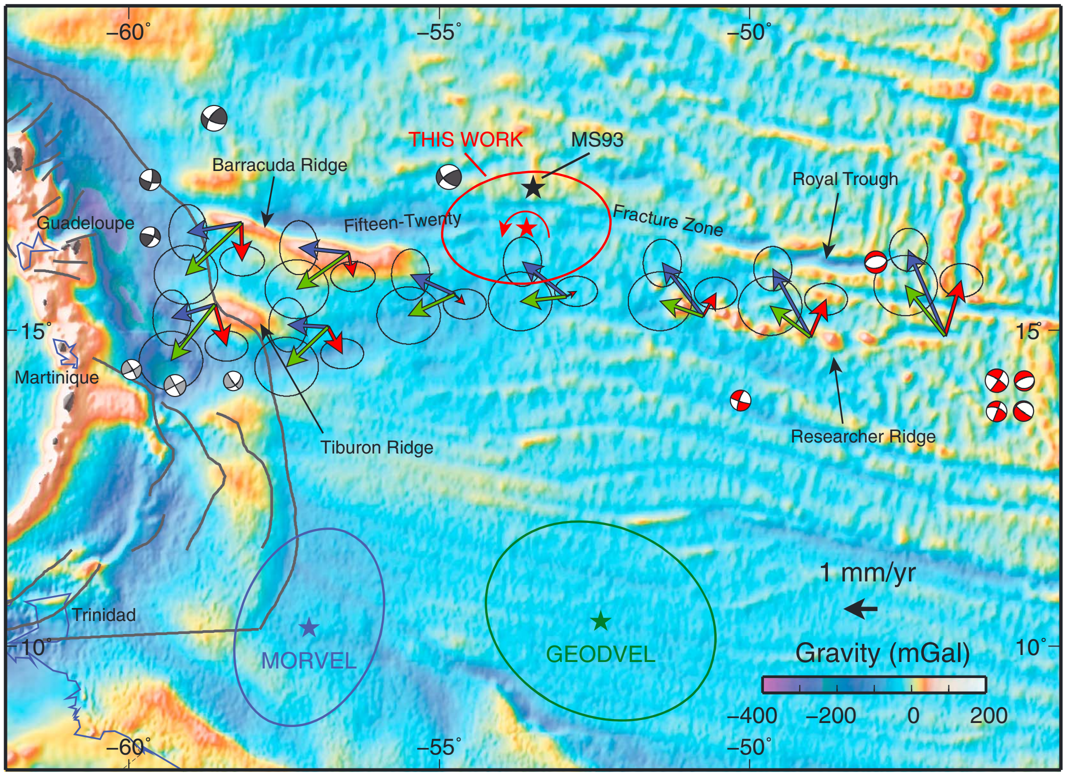

Figure 12. Predicted motion of the North American plate relative to South America along their common boundary in the central western Atlantic. Red shows this work, blue shows *DeMets et al.* [2010], green shows *Argus et al.* [2010], black shows 0–10.4 Ma stage pole from *Müller and Smith* [1993]. Background shows free-air gravity anomalies from *Sandwell and Smith* [2009].

portion of the plate boundary-parallel slip could be accommodated by the shallow Bowin and Bunce faults on the inner wall of the Puerto Rico trench [*Grindlay et al.*, 2005b; *ten Brink and Lin*, 2004]. The partitioning of the oblique convergence between the Caribbean and North American plates into plate interface convergence and intra-arc strike-slip faulting, therefore, ceases as the plate boundary transitions from the oblique collision of the Bahamas platform with Hispaniola to the oblique subduction of old (> 100 Ma) lithosphere under Puerto Rico [*Dolan et al.*, 1998; *Mann et al.*, 2002; *Grindlay et al.*, 2005a; *Mondziel et al.*, 2010].

The model predicts little motion (<1.4 mm/yr) across the Anegada Passage fault system while the relative motion between the arc and the North American plate remains constant in direction and magnitude. This holds all the way down the Lesser Antilles arc, where velocity residuals with respect to the Caribbean plate are within measurement errors at all reliable GPS sites (see section 4 above). This is also true for site BDOS on Barbados island, which has a 9 year continuous observation time span and is located on the emerged part of the old Antilles accretionary prism [*Bangs et al.*, 2003]. The GPS data are not consistent with the 5 mm/yr motion of a northern Lesser Antilles rigid sliver proposed by *Lopez et al.* [2006]. They also exclude the slip partitioning model proposed by *Feuillet et al.* [2002, 2010] with 5 to 10 mm/yr of distributed deformation throughout the northern Lesser Antilles. The observed active faults within the arc and forearc must therefore be accumulating strain at a rate of at most 1–2 mm/yr, the average residual of the best fit model in the Lesser Antilles.

Along the southern boundary of the Caribbean plate, the best fit model predicts pure strike-slip motion on the El Pilar fault in northern Venezuela at ~18 mm/yr. Farther west the Caribbean/South America relative motion splits into 1.5 mm/yr of pure strike-slip motion on the Oca fault and 2–2.5 mm/yr on the left-lateral Santa Marta-Bucaramanga fault, while the bulk of the plate motion is accommodated by ~12 mm/yr of right-lateral strike slip on the Bocono fault. Consistent with previous results, the Bocono fault also accommodates up to 3 mm/yr of shortening. The left-lateral strike-slip motion predicted by the model along the Santa Marta-Bucaramanga faults is at the low end of slip rate estimates from maximum ages of Quaternary offset features (0.2 mm/yr) [*Paris et al.*, 2000], paleoseismological studies at its northern termination (5–15 mm/yr)

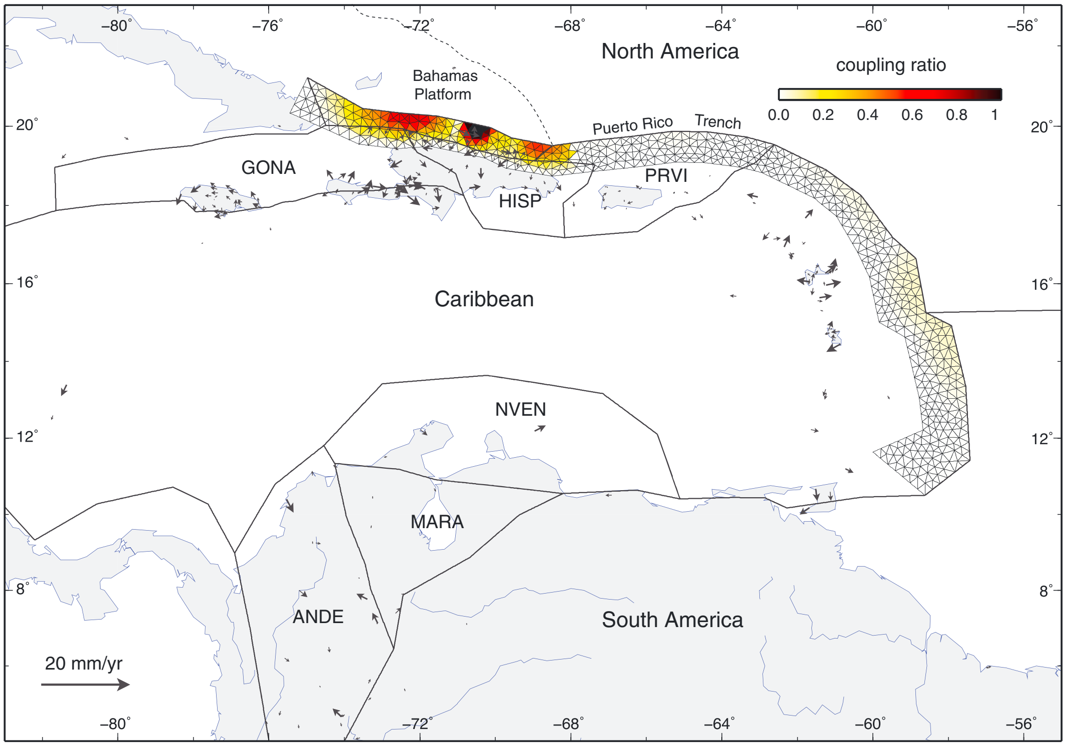

Figure 13. Coupling ratio estimated along the Greater-Lesser Antilles subduction interface estimated on the discretized plate interface also shown in Figure 4. Residual velocities are shown with black arrows. We omitted their error ellipses for a sake of readability. The thin dashed line indicates the boundary of the Bahamas Platform. Note the coincidence between the transition from coupled to uncoupled plate interface with the transition from Bahamas Platform collision to oceanic subduction at the Puerto Rico trench.

[*Diederix et al.*, 2012; *Idarraga-Garia and Romero*, 2010], or earlier GPS results (6 ± 2 mm/yr) [*Trenkamp et al.*, 2002]. The model slip rate for the Bocono fault is consistent with estimates of right-lateral strike-slip motion from paleoseismological investigations [*Audemard et al.*, 1999, 2005]. The model predicts ∼N-S convergence across the South Caribbean Deformed Belt at ∼3 mm/yr offshore northeastern Venezuela, transitioning to ∼5 mm/yr offshore central Venezuela, and ∼8 mm/yr offshore northern Colombia. These values are, however, not very robust because of the limited number of GPS sites available on the north Venezuela and Andes blocks.

Finally, we find a rotation pole for the relative motion between North and South America located in the central part of the Fifteen-Twenty Fracture Zone (Figure 12), close to the stage pole found by [*Müller and Smith*, 1993] for the 0–10.4 Ma period (17.2° latitude, −53.5° longitude), with a similar rotation rate (0.2°/Ma). This indicates that the South America-North America relative motion has not varied significantly over the past∼10 Ma. Our model predicts about 1 mm/yr of present-day N-S shortening across the Barracuda and Tiburon ridges to the west, consistent with offshore geological data showing thrusting and thrust-related folding affecting Quaternary sediments along both ridges indicative of north-south compression [*Patriat et al.*, 2011]. This prediction is in closer agreement with geological observations there than other recent estimates [*DeMets et al.*, 2010; *Argus et al.*, 2010] that predict a significant amount of strike-slip motion that does not appear in the offshore geological data [*Pichot et al.*, 2012]. Our South America-North America rotation parameters also predicts up to 1 mm/yr of N-S plate divergence to the east, consistent with extension at the Royal trough [*Roest and Collette*, 1986] (see also one CMT focal mechanism at the Royal trough in Figure 12) and with a cluster of anomalous focal mechanisms off the mid-Atlantic ridge to the south and east that show N-S directed *T* axes [*Escartin et al.*, 2003].

4.2. Low Coupling on the Lesser Antilles Subduction

A robust and important output of the block models is the very low coupling estimated along the Lesser Antilles and Puerto Rico subduction interface (Figure 13). Taken at face value, this would indicate that the 19 mm/yr of plate convergence builds little to no slip deficit on the plate interface (Table 3). As for many subduction, GPS

Table 3. Slip Deficit Rates in mm/yr for Major Faults (Minimum and Maximum Strike-Slip and Dip-Slip Values Are Provided) for the Best Fit Model and for a Model With the Same Geometry Where Full Locking Is Enforced at the Greater-Lesser Antilles Subduction

	Best Fit Model				Locked Subduction				Uncertainties	
	Strike Slip		Dip Slip		Strike Slip		Dip Slip			
Faults	max	min	max	min	max	min	max	min	σ_{SS}	σ_{DS}
Oriente fault	10.3	8.9	0	0	10.3	8.9	0	0	0.4	0.0
Septentrional Haiti	10	8.8	0	0	10.0	8.8	0	0	0.7	0
Septentrional D.R.	10.1	9.7	0	0	10.1	9.7	0	0	0.7	0
South Jamaica	9.4	5.7	0	0	9.4	8.7	0	0	0.3	0
EPGF Haiti	10.3	8.1	0	0	10.3	8.1	0	0	0.3	0.0
Muertos West	4.9	1.5	13.7	5.1	4.9	1.5	13.7	5.1	0.5	0.5
Muertos East	0.4	0	1.5	0	0.4	0	1.5	0	0.4	0.5
Anegada Passage	0.5	0.3	0	0	0.5	0.3	0	0	0.5	0.0
Mona Passage	2.3	0.3	0	0	2.3	0.3	0	0	0.8	0.0
North Hispaniola	3.1	0	4.2	2.5	1.2	0.4	4.6	1.5	0.8	1.2
Puerto Rico trench	0.3	0	1.0	0.2	15.5	12.6	12.8	3.3	0.5	0.7
Lesser Antilles N	0.3	0	2.2	1.2	12.8	2.6	19.2	13.6	0.2	0.4
Lesser Antilles S	0.3	0	3.1	2.3	18.5	0.6	20.2	8.5	0.3	0.3
El Pilar fault	20.3	15.9	0	0	20.3	15.9	0	0	0.5	0.0
Oca fault	1.5	1.2	0	0	1.5	1.2	0	0	1.0	0.0
Bocono fault	12.7	10.9	0	0	12.7	10.9	0	0	0.8	0.0
Santa Marta fault	2.3	2	0	0	2.3	2	0	0	0.7	0.0
Venezuela thrust	3.2	0.2	5.3	0.3	3.2	0.2	5.3	0.3	1.6	1.6
Colombia thrust	5.6	0.8	9.8	5.4	5.6	0.8	9.8	5.4	0.9	0.9

measurements on the island arc provide limited coverage of the plate interface, in particular at close distance to the trench. Trench to Island Arc distances, ranging from 175 to 250 km with a depth of the subduction interface beneath the arc ranging from 50 to 100 km, are however similar to Japan or South America, where locked sections of the plate interface do show strain accumulation at coastal GPS stations [e.g., *Mazzotti et al.*, 2000; *Loveless and Meade*, 2010; *Nocquet et al.*, 2014].

As discussed above, the fact that the velocities of Lesser Antilles GPS sites are consistent with the stable Caribbean plate suggests a plate interface that is at least only partially coupled. This is shown on cross sections across the central (Guadeloupe), northern (St Martin), and southern (Barbados) parts of the subduction (Figure 14) which compare the arc deformation predicted by the best fit model to that predicted using a plate interface fully locked to 40 km depth. It is apparent in Figure 14 that a fully locked plate interface would cause measurable deformation of the arc, in particular at the Desirade (Guadeloupe, site ADE0), St. Martin (site SMRT), and Barbados (site BDOS). These sites, as well as the ones more distal to the trench, show no evidence of elastic strain accumulation.

We ran resolution tests in order to determine the spatial resolution of the coupling ratio along the plate interface allowable by the data (Figure 15). To do so, we calculated slip rates on the subduction patches using the best fit block model and prescribed either full locking (i.e., slip rate = full relative plate motion) or no locking (i.e., slip rate = 0) in a forward model where we calculate predicted velocities at all GPS sites. We kept the same geometry as the best fit model for all synthetic models unless specified. We perturbed the predicted velocity using Gaussian white noise with a standard deviation of 0.5 mm/yr, consistent with the RMS scatter of the data to the block model. We then used this predicted velocity field, together with the observed velocity uncertainties, to solve for both rigid block motion and slip on the subduction patches.

We first seek to determine whether the data can resolve the lateral variation in the slip rate estimate in the best fit model, from 0 mm/yr north of Hispaniola (i.e., fully coupled plate interface) to close to the full relative plate motion rate along the Puerto Rico and Lesser Antilles subduction (i.e., uncoupled plate interface). We run three successive models where we prescribe uniform slip on the North Hispaniola fault (3 mm/yr),

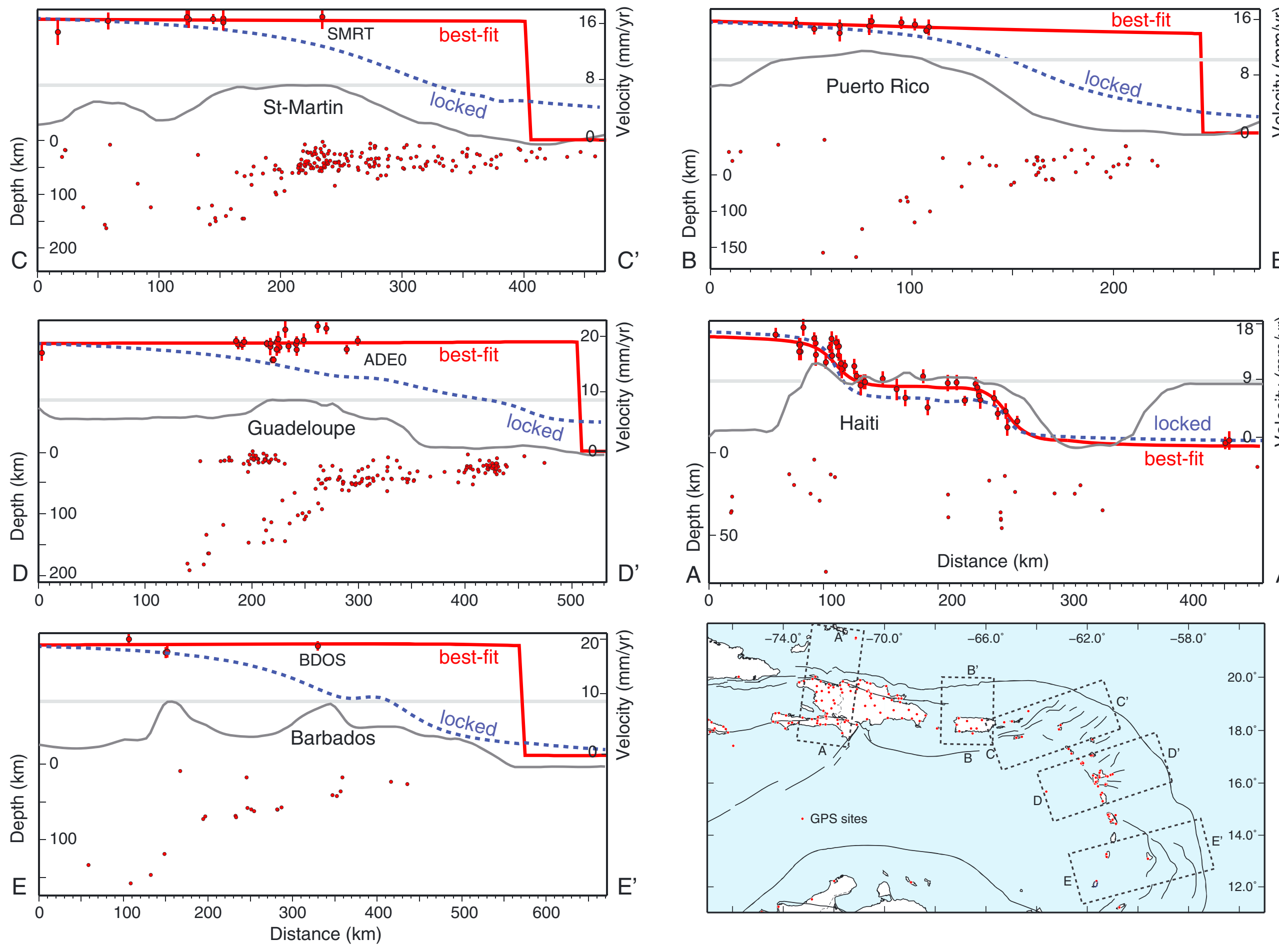

Figure 14. Sections across the Lesser and Greater Antilles subduction showing topography (grey line), earthquake hypocenter [*Engdahl et al.*, 1998], velocity magnitude at the GPS sites (red circles with 95% confidence error bar), velocity predicted by the best fit model (solid red line), and velocity predicted by a forward model where we impose full coupling on the subduction interface (dashed blue line). The misfit of the data to a fully locked plate interface is apparent on the three Lesser Antilles cross sections.

Puerto Rico subduction (19 mm/yr), and Lesser Antilles subduction (19 mm/yr) (Figures 15a–15c). As shown in Figures 15d–15f, the data allow for the recovery of this spatial variability with some smearing at the segment edges. This shows that the transition from locked to unlocked from Hispaniola to Puerto Rico is resolvable by the data. It also shows that the data are sufficient to detect fully locked plate interfaces along each of the Hispaniola, Puerto Rico, and Lesser Antilles subduction segments. A similar test with alternating locked/unlocked segments of shorter length (~200 km, Figures 15g and 15j) shows that the data can resolve small-scale variability on the North Hispaniola thrust but with significant smearing and poor resolution along the Puerto Rico and Lesser Antilles subduction segments.

We then seek to determine how well the available data can resolve along-dip variations in interplate coupling. To do so, we impose full locking or unlocking along the upper or lower half of the subduction interface. As shown in Figures 15h–k and 15i–l, the downdip resolution of the models is poor, a consequence of the distribution of sites on the island arc at more than 200 km from the subduction trench. We then ask whether offshore geodetic sites could improve the along-dip resolution of the estimated coupling and how many would be needed. We placed fictitious offshore sites at various distances to the trench and ran a series of tests where we impose full locking on the lower half of the subduction interface (Figure 16a). As expected, the resulting resolution varies greatly with the number of sites and their distribution. With 20 GPS sites uniformly distributed on top of the subduction interface, we obtain a good along-dip resolution with some smearing in regions where the space between the GPS sites become large. The resolution is still acceptable with 10 GPS sites (Figure 16d) and becomes poor with five only sites.

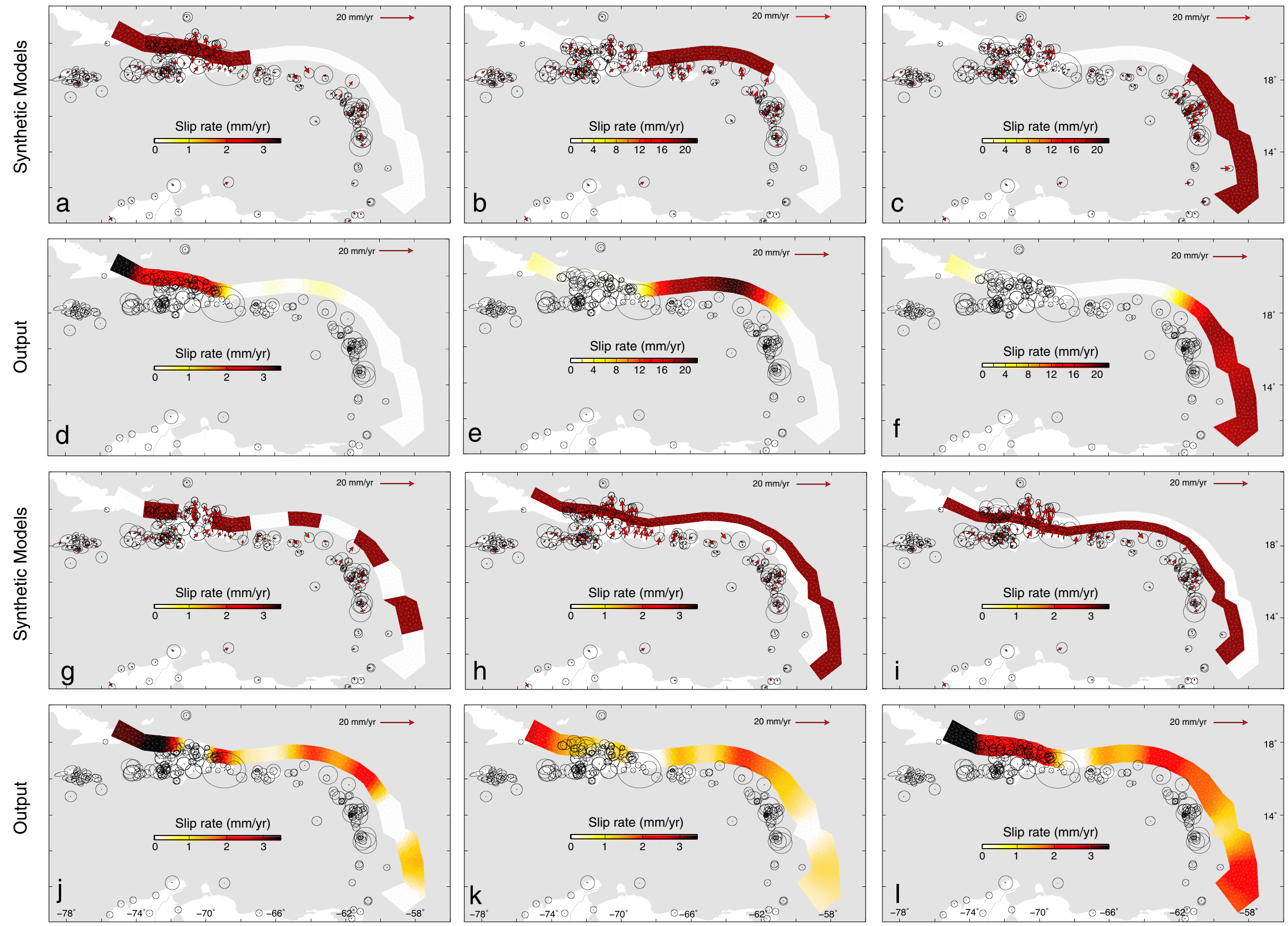

Figure 15. Tests of the ability of the data to resolve lateral and depth-dependent variations in coupling along the Greater-Lesser Antilles subduction plate interface. (a–c and g–i) Input synthetic forward models. (d–f and j–l) Corresponding outputs from an inversion using the velocities predicted by the forward model. It is readily apparent that the data distribution allows us to determine lateral variations in plate coupling with confidence, but that depth-dependent variations are poorly constrained by the data.

We conclude that low coupling (0–10%) along the Lesser Antilles/Puerto Rico section of the Caribbean-North America plate interface is a robust feature of the model, although one cannot determine the depth distribution of coupling with confidence. *Stein et al.* [1982] first pointed out the lack of significant thrust faulting earthquakes ($M > 7$) in the Lesser Antilles in the historical and instrumental record, which they interpreted as indicative of an uncoupled and aseismic subduction where *only a small fraction of the slip occurs as interface thrust earthquakes*. Although there are a few moderate magnitude ($4 < M < 6.5$) thrust events on, or close to, the plate interface, all magnitude greater than 6.5 events in the region have a normal faulting mechanism (Figure 1). This holds in particular for the four largest earthquakes in the historical record (M_s7.5 1953; M_s7.5 1969; M_s7.4 1974; and M_w7.4 2007) which are all normal faulting events within the subducting slab. Interestingly, the most recent significant earthquakes in the region (16 May 2014 M_w5.9 and 18 February 2014 M_w6.5) are also normal faulting events that occurred in the distal part of the accretionary prism (close to the trench) at depths of 12 and 14 km, respectively. According to the seismic refraction profile reported in *Kopp et al.* [2011], these extensional events could have occurred in the lowermost part of the accretionary wedge.

The largest historical earthquakes in the Lesser Antilles in 1690 and 1843 [*Robson*, 1964] are both reported to have reached an intensity of 10 [*Dorel*, 1981]. The magnitude of the better documented 1843 event has been estimated 7.5 to 8.0 [*Bernard and Lambert*, 1988; *ten Brink et al.*, 2011], 8.0 to 8.5 [*McCann et al.*, 1982], 8.5 [*Feuillet et al.*, 2001], or greater than 8.5 [*Hough*, 2013]. Because of its magnitude and location at a subduction plate boundary, this earthquake, which did not cause a tsunami, is often interpreted as a thrust event on the plate interface [*McCann and Sykes*, 1984b; *Bernard and Lambert*, 1988] though no direct evidence for this is

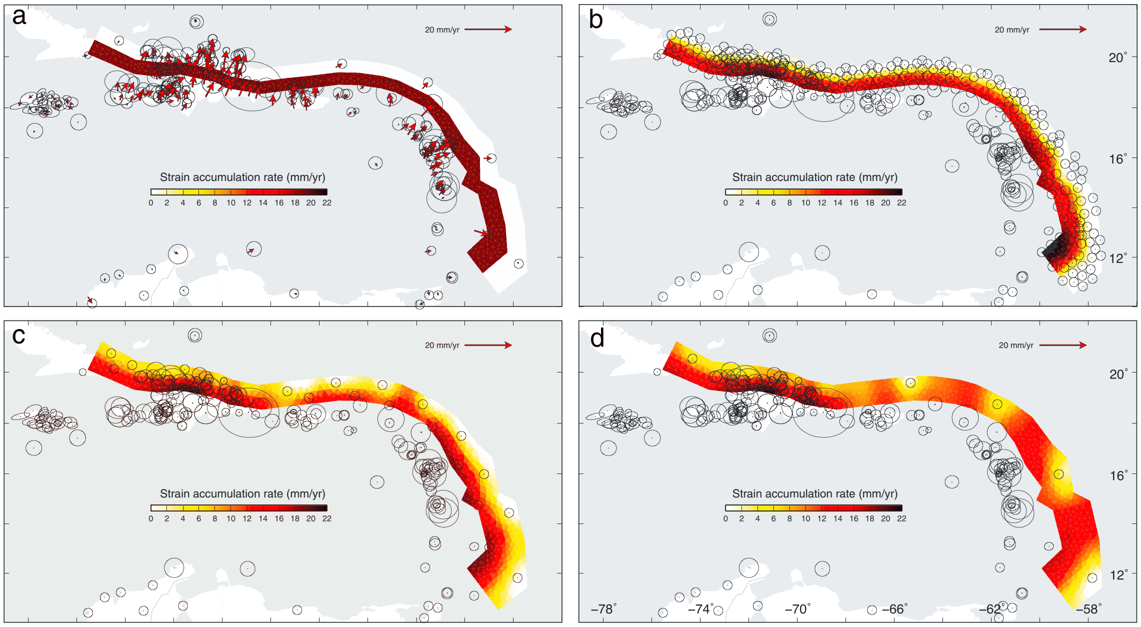

Figure 16. (a) Synthetic forward model and recovered slip distribution adding (b) 100, (c) 20, or (d) 10 fictitious offshore GPS sites to the existing GPS sites used in this study.

available. If this event is indeed a thrust, then the very low slip deficit on the subduction interface inferred from GPS data implies that similar events have a long recurrence time. Using the empirical relations between average slip and moment magnitude [*Wells and Coppersmith*, 1994], we find a recurrence time of 2000 years for M_w8.0 events and 3 mm/yr of average slip on the subduction interface. Alternatively, the 1843 event may have had a source mechanism similar to its large normal faulting neighboring events of 1969 (M_s7.5), 1974 (M_s7.4), and 2007 (M_w7.4). A similar depth range of 40–140 km would explain the lack of a tsunami and the lack of substantial coseismic uplift reported [*Bernard and Lambert*, 1988].

The low coupling inferred here for the Lesser Antilles subduction bears similarities with a similar result at the Hellenic subduction, where *Vernant et al.* [2014] find that strain accumulation on the plate interface accommodates <20% of the Nubia-Aegean convergence rate. The context is interestingly similar, with a ~900 km long arcuate subduction, a slow convergence rate (~3 cm/yr), and the subduction of old (>100 Myr) and dense oceanic crust. Slab-pull and rollback of the subduction have been invoked as a mechanism that reduces the normal stress acting on the plate interface and facilitates aseismic slip [*Scholz and Campos*, 1995]. This mechanism would be consistent with the pervasive normal faulting documented throughout the northern half of the Lesser Antilles arc [*Feuillet et al.*, 2002]. Alternatively, *Wallace et al.* [2012b] propose that fluid overpressure, because it reduces frictional strength of faults, lowers the depth of the transition from frictional to viscous behavior. As a consequence, subduction zones experiencing significant fluid overpressure should be locked to greater depths than those where high permeability prevents overpressure to develop. These authors propose that the former (e.g., highly overpressured, deep locking) would occur in regions of upper plate contractional tectonics, while the latter (e.g., more permeable upper plate, less overpressure, and shallower locking depths) would correspond to an extensional stress regime in the forearc. A correlation is indeed observed between along-strike transition from locked to creeping subduction and a coincidental transition from compressional to extensional stress regime in the upper plate in New Zealand, Japan, and Vanuatu. The same observation holds in the Caribbean, where the transition from upper plate contraction to extension between Hispaniola and Puerto Rico also corresponds to the transition from deep interseismic locking to aseismic creep on the plate interface. Mechanical models, beyond the scope of the present study, are now needed to test this hypothesis.

The Lesser Antilles subduction has been compared with the Tohoku segment of the Japan subduction, which ruptured on 11 March 2011 in a M_w9.3 earthquake. Both share seismicity in the mantle wedge (mostly normal faulting) and thrust events at the plate interface just below the mantle wedge [*Laigle et al.*, 2013]. Recent studies show that the Tohoku rupture may have extended under the mantle wedge, which somewhat broadens the width of the seismogenic zone [*Koketsu et al.*, 2011]. However, full and deep interseismic coupling was documented by GPS measurements along the Tohoku segment before the March 2011 earthquake [*Mazzotti et al.*, 2000; *Loveless and Meade*, 2010], a characteristic that is opposite to the findings reported here for the Lesser Antilles subduction.

5. Conclusions

We have assembled an up-to-date GPS velocity field for the Caribbean plate and its boundaries with North and South America which we used to quantify the kinematics of active deformation in the region. Our results confirm several earlier findings, in particular for the Caribbean-North America plate boundary, and extend them to the Lesser Antilles and the Caribbean-South America boundary. A new key finding is the low coupling required by the GPS data along the Lesser Antilles subduction interface, which was previously poorly resolved.

As a consequence, seismic hazard associated with strike-slip plate boundary faults along the northern and southern margins of the Caribbean plate is at least as important as the threat posed by the subduction plate interface in the Lesser Antilles. This seems to be reflected in the distribution of large historical earthquakes in the region [*Stein et al.*, 1982]. Under the paradigm that the magnitude of large earthquakes depends on the slip deficit accumulated on a potential rupture of sufficient area, the very low seismogenic coupling found here on the Lesser Antilles subduction allows at most one *M*8 earthquake every 2000 years, or one Tohoku-size event every 3500 years.

The limited coverage of GPS measurements in the region calls for additional sites where still possible, though significant progress has been made in the framework of the COCONet initiative [*Braun et al.*, 2012]. Given the oceanic nature of most of the Caribbean plate boundaries, offshore geodesy appears to be a viable way forward, though the implementation cost may be large. In addition, systematic efforts to obtain a reliable catalog of paleoearthquakes in the region is the key to our understanding of the regional seismic and tsunami hazard.

Acknowledgments
We thank the agencies and individuals that made GPS data collection possible in the Dominican Republic (Direccion General de Mineria the Institut Cartografico Militar, Colegio Dominicano de Ingenieros, Arquitectos y Agrimensores, Holasa S.A.) and Haiti (Bureau des Mines et de l'Energie, Direction de la Protection Civile, Centre National de l'Information Géo-Spatiale, Faculté des Sciences de Université d'Etat). We thank the teams from the Observatoires Volcanologiques et Sismologiques of Guadeloupe (OVSG) and Martinique (OVSM) and from the Institut de Physique du Globe de Paris (IPGP) for their relentless work over the years installing, maintaining, and monitoring permanent and episodic GPS stations and participating in the data processing. We are grateful to Jack Loveless for his support with the kinematic modeling code blocks and thank the Associate Editor, Philippe Vernant, and Paul Mann for their constructive comments that helped improved the manuscript. This research is supported by a COCONet fellowship from UNAVCO to S.S. and National Science Foundation awards EAR-0409487, EAR-RAPID-1024990, and EAR-1045809 to E.C. This work uses data services provided by the UNAVCO Facility with support from the U.S. National Science Foundation (NSF) and National Aeronautics and Space Administration (NASA) under NSF Cooperative Agreement EAR-0735156. Permanent and episodic GPS within the OVSG, OVSM, and IPGP footprint in the Lesser Antilles have been funded by CNRS-INSU-ACI programs originally, then through two FEDER European Community programs (CPER-PO and Interreg IV Caraïbe projects) cofunded by the French Ministry of Research, the French Ministry of Environment, the Guadeloupe Regional Council, and the IPGP. We thank the IGS and its centers for providing open GNSS data and data products to the community. All data used in this work are openly available from the IGS (igscb.jpl.nasa.gov) and UNAVCO (www.unavco.org) archives. Ancillary information necessary to process GPS data, such as precise satellite orbits and antenna phase center models, is openly available from the IGS (igscb.jpl.nasa.gov). Global SINEX files used here are publicly available at MIT (acc.igs.org/reprocess.html). The software used to process the GPS data (GAMIT-GLOBK) is openly available at MIT (www-gpsg.mit.edu/-simon/gtgk). Figures were produced using the Generic Mapping Tools software package [*Wessel and Smith*, 1998]. Measurement campaigns in the Lesser Antilles used services of the French INSU-CNRS GPS instrument pool.

References

Altamimi, Z., X. Collilieux, and L. Métivier (2011), Itrf2008: An improved solution of the international terrestrial reference frame, *J. Geod.*, *85*(8), 457–473.

Argus, D. F., R. G. Gordon, M. B. Heflin, C. Ma, R. J. Eanes, P. Willis, W. R. Peltier, and S. E. Owen (2010), The angular velocities of the plates and the velocity of Earth's centre from space geodesy, *Geophys. J. Int.*, *180*(3), 913–960.

Audemard, F., D. Pantosti, M. Machette, C. Costa, K. Okumura, H. Cowan, H. Diederix, and C. Ferrer (1999), Trench investigation along the Mérida section of the Boconó fault (central Venezuelan Andes), Venezuela, *Tectonophysics*, *308*(1), 1–21.

Audemard, F., M. Machette, J. Cox, R. Dart, and K. Haller (2000), Map and database of quaternary faults and folds in Venezuela and its offshore regions, *USGS Open-File Rep. 00-0018*, 78 p., xcale 1:2,000,000, Regional Coord.: Carlos Costa, Univ. San Luis–Argentina, ILP II-2 co-chairman Western Hemisphere: Michael Machette, USGS-Colorado.

Audemard, F. A., G. Romero, H. Rendon, and V. Cano (2005), Quaternary fault kinematics and stress tensors along the southern Caribbean from fault-slip data and focal mechanism solutions, *Earth Sci. Rev.*, *69*(3–4), 181–233.

Babb, S., and P. Mann (1999), Structural and sedimentary development of a neogene transpressional plate boundary between the Caribbean and South America plates in Trinidad and the Gulf of Paria, in *Sedimentary Basins of the World*, vol. 4, pp. 495–557, Elsevier, Amsterdam.

Bakun, W. H., C. H. Flores, and S. Uri (2012), Significant earthquakes on the Enriquillo fault system, Hispaniola, 1500–2010: Implications for seismic hazard, *Bull. Seismol. Soc. Am.*, *102*(1), 18–30.

Bangs, N. L., G. L. Christeson, and T. H. Shipley (2003), Structure of the Lesser Antilles subduction zone backstop and its role in a large accretionary system, *J. Geophys. Res.*, *108*(B7), 2358, doi:10.1029/2002JB002040.

Benford, B., C. DeMets, and E. Calais (2012a), GPS estimates of microplate motions, northern Caribbean: Evidence for a Hispaniola microplate and implications for earthquake hazard, *Geophys. J. Int.*, *191*(2), 481–490.

Benford, B., C. DeMets, B. Tikoff, P. Williams, L. Brown, and M. Wiggins-Grandison (2012b), Seismic hazard along the southern boundary of the Gônave microplate: Block modelling of GPS velocities from Jamaica and nearby islands, northern Caribbean, *Geophys. J. Int.*, *190*(1), 59–74.

Bernard, P., and J. Lambert (1988), Subduction and seismic hazard in the northern Lesser Antilles: Revision of the historical seismicity, *Bull. Seismol. Soc. Am.*, *78*(6), 1965–1983.

Braun, J. J., et al. (2012), Focused study of interweaving hazards across the Caribbean, *Eos Trans. AGU*, *93*(9), 89–90.

Byrne, G. D., W. Suarez, and W. R. McCann (1985), Muertos trough subduction-microplate tectonics in the northern Caribbean?, *Nat. Geosci.*, *317*(6036), 420–421.

Calais, E., and B. M. de Lépinay (1990), A natural model of active transpressional tectonics the enéchelon structures of the Oriente deep, along the northern Caribbean transcurrent plate boundary (southern Cuban Margin), *Oil Gas Sci. Technol.*, *45*(2), 147–160.

Calais, E., and B. M. de Lepinay (1991), From transtension to transpression along the northern Caribbean plate boundary off Cuba: Implications for the recent motion of the Caribbean plate, *Tectonophysics*, *186*(3–4), 329–350.

Calais, E., and B. M. de Lépinay (1992), The northern Caribbean transcurrent plate boundary in Hispaniola: Paleogeographic and structural evolution during the Cenozoic, *Bull. De La Soc. Geol. De France*, *163*, 309–324.

Calais, E., N. Béthoux, and B. M. Lépinay (1992), From transcurrent faulting to frontal subduction: A seismotectonic study of the northern Caribbean plate boundary from Cuba to Puerto Rico, *Tectonics*, *11*(1), 114–123.

Calais, E., Y. Mazabraud, B. M. de Lépinay, P. Mann, G. Mattioli, and P. Jansma (2002), Strain partitioning and fault slip rates in the northeastern Caribbean from GPS measurements, *Geophys. Res. Lett.*, *29*(18), 1856, doi:10.1029/2002GL015397.

Calais, E., J. Han, C. DeMets, and J. Nocquet (2006), Deformation of the North American plate interior from a decade of continuous GPS measurements, *J. Geophys. Res.*, *111*, B06402, doi:10.1029/2005JB004253.

Calais, E., Freed A., G. Mattioli, F. Amelung, S. F. J. Jónsson, P. Jansma, S.-H. Hong, T. Dixon, C. P. Prépetit, and R. Momplaisir (2010), Transpressional rupture of an unmapped fault during the 2010 Haiti earthquake, *Nat. Geosci.*, *3*(11), 794–799.

Chlieh, M., H. Perfettini, H. Tavera, J.-P. Avouac, D. Remy, J.-M. Nocquet, F. Rolandone, F. Bondoux, G. Gabalda, and S. Bonvalot (2011), Interseismic coupling and seismic potential along the Central Andes subduction zone, *J. Geophys. Res.*, *116*, B12405, doi:10.1029/2010JB008166.

Cubas, N., J. -P. Avouac, P. Souloumiac, and Y. Leroy (2013), Megathrust friction determined from mechanical analysis of the forearc in the Maule earthquake area, *Earth Planet. Sci. Lett.*, *381*, 92–103.

DeMets, C., and T. H. Dixon (1999), New kinematic models for Pacific-North America motion from 3 Ma to present. I: Evidence for steady motion and biases in the NUVEL-1A model, *Geophys. Res. Lett.*, *26*(13), 1921–1924.

DeMets, C., R. G. Gordon, D. F. Argus, and S. Stein (1994), Effect of recent revisions to the geomagnetic reversal time scale on estimates of current plate motions, *Geophys. Res. Lett.*, *21*(20), 2191–2194.

DeMets, C., P. E. Jansma, G. S. Mattioli, T. H. Dixon, F. Farina, R. Bilham, E. Calais, and P. Mann (2000), Gps geodetic constraints on Caribbean-North America plate motion, *Geophys. Res. Lett.*, *27*(3), 437–440.

DeMets, C., R. G. Gordon, and D. F. Argus (2010), Geologically current plate motions, *Geophys. J. Int.*, *181*(1), 1–80.

Dewey, J. W. (1972), Seismicity and tectonics of western Venezuela, *Bull. Seismol. Soc. Am.*, *62*(6), 1711–1751.

Diederix, H., C. Hernández, E. Torres, J. A. Osorio, and P. Botero (2012), Resultados preliminares del primer estudio paleosismológico a lo largo de la falla de Bucaramanga, Colombia, *Ingeniería Investigación y Desarrollo*, *9*(2), 1–3.

Dillon, W. P., N. T. Edgar, K. M. Scanlon, and D. F. Coleman (1996), A review of the tectonic problems of the strike-slip northern boundary of the Caribbean plate and examination by GLORIA, in *Geology of the United States' Seafloor: The View From GLORIA*, edited by J. V. Gardner, M. E. Field, and D. C. Twichell, pp. 135–164, Cambridge Univ. Press, London, U. K.

Dixon, T. H., F. Farina, C. DeMets, P. Jansma, P. Mann, and E. Calais (1998), Relative motion between the Caribbean and North American plates and related boundary zone deformation from a decade of GPS observations, *J. Geophys. Res.*, *103*(B7), 15,157–15,182.

Dolan, J., and D. J. Wald (1998), The 1943–1953 north-central Caribbean earthquakes: Active tectonic setting, seismic hazards, and implications for Caribbean-North America plate motions, in *Active Strike Slip and Collisional Tectonic Setting, Seismic Hazards, and Implications for Caribbean-North America Plate Motions*, edited by J. F. Dolan and P. Mann, pp. 143–169, Geol. Soc. Of Am., Boulder, Colo.

Dolan, J. F., and D. D. Bowman (2004), Tectonic and seismologic setting of the 22 September 2003, Puerto Plata, Dominican Republic earthquake: Implications for earthquake hazard in Northern Hispaniola, *Seismol. Res. Lett.*, *75*(5), 587–597.

Dolan, J. F., H. T. Mullins, and D. J. Wald (1998), Active tectonics of the north-central caribbean: Oblique collision, strain partitioning, and opposing subducted slabs, in *Active Strike-Slip and Collisional Tectonics of the Northern Caribbean Plate Boundary Zone*, pp. 1–62, Special Papers-Geol. Soc. Of Am., Boulder, Colo.

Dorel, J. (1981), Seismicity and seismic gap in the lesser antilles arc and earthquake hazard in Guadeloupe, *Geophys. J. Int.*, *67*(3), 679–695.

Ekstrom, G., M. Nettles, and A. M. Dziewoński (2012), Physics of the Earth and Planetary Interiors, *Phys. Earth Planet. Inter.*, *200-201*(C), 1–9.

Engdahl, E. R., R. van der Hilst, and R. Buland (1998), Global teleseismic earthquake relocation with improved travel times and procedures for depth determination, *Bull. Seismol. Soc. Am.*, *88*(3), 722–743.

Escartin, J., D. Smith, and M. Cannat (2003), Parallel bands of seismicity at the mid-Atlantic ridge, 12–14°N, *Geophys. Res. Lett.*, *30*(12), 1620, doi:10.1029/2003GL017226.

Feuillet, N., I. Manighetti, and P. Tapponnier (2001), Active extension perpendicular to subduction in the Lesser Antilles island arc; Guadeloupe, French Antilles, *CR Acad. Sci., Ser. II*, *333*(9), 583–590.

Feuillet, N., I. Manighetti, P. Tapponnier, and E. Jacques (2002), Arc parallel extension and localization of volcanic complexes in Guadeloupe, Lesser Antilles, *J. Geophys. Res.*, *107*(B12), 2331, doi:10.1029/2001JB000308.

Feuillet, N., et al. (2010), Active faulting induced by slip partitioning in Montserrat and link with volcanic activity: New insights from the 2009 GWADASEIS marine cruise data, *Geophys. Res. Lett.*, *37*, L00E15, doi:10.1029/2010GL042556.

Frankel, A., W. R. McCann, and A. J. Murphy (1980), Observations from a seismic network in the Virgin Islands region: Tectonic structures and earthquake swarms, *J. Geophys. Res.*, *85*(B5), 2669–2678.

Gestel, J. -P., P. Mann, J. F. Dolan, N. R. Grindlay, and Structure and tectonics of the upper Cenozoic Puerto Rico-Virgin islands carbonate platform as determined from seismic reflection studies (1998), *J. Geophys. Res.*, *103*(B12), 30,505–30,530.

Graham, S. E., C. Demets, H. R. DeShon, R. Rogers, M. R. Maradiaga, W. Strauch, K. Wiese, and D. Hernandez (2012), GPS and seismic constraints on the M = 7.3 2009 Swan Islands earthquake: Implications for stress changes along the Motagua fault and other nearby faults, *Geophys. J. Int.*, *190*(3), 1625–1639.

Granja Bruña, J., A. Carbó-Gorosabel, P. Llanes Estrada, A. Muñoz-Martín, U. ten Brink, M. Gómez Ballesteros, M. Druet, and A. Pazos (2014), Morphostructure at the junction between the Beata Ridge and the Greater Antilles island arc (offshore Hispaniola southern slope), *Tectonophysics*, *618*, 138–163.

Granja Bruña, J. L., U. S. Ten Brink, A. Carbó-Gorosabel, A. Muñoz-Martín, and M. Gómez Ballesteros (2009), Morphotectonics of the Central Muertos thrust belt and muertos trough (Northeastern Caribbean), *Mar. Geol.*, *263*(1), 7–33.

Grindlay, N., P. Mann, and J. Dolan (1997), Researchers investigate submarine faults north of Puerto Rico, *Eos. Trans. AGU*, *78*(38), 404–404.

Grindlay, N., L. Abrams, L. Del Greco, and P. Mann (2005a), Toward an integrated understanding of Holocene fault activity in Western Puerto Rico: Constraints from high-resolution seismic and sidescan sonar data, in *Active Tectonics and Seismic Hazards of Puerto Rico, the Virgin Islands, and Offshore Areas*, edited by P. Mann, *Geol. Soc. Am. Spec. Pap.*, *385*, 139–160.

Grindlay, N. R., M. Hearne, and P. Mann (2005b), High risk of tsunami in the northern Caribbean, *Eos. Trans. AGU*, *86*(12), 121–126.

Gutscher, M. -A., G. K. Westbrook, B. Marcaillou, D. Graindorge, A. Gailler, T. Pichot, and R. C. Maury (2010), *Along Strike Variations in the Width of the Seismogenic Zone of the Lesser Antilles Subduction Predicted by Thermal Modeling*, Vienna, Austria, 2–7 May, vol. 12.

Hayes, G., et al. (2010), Complex rupture during the 12 January 2010 Haiti earthquake, *Nat. Geosci.*, *3*(11), 800–805.

Hayes, G. P., D. E. McNamara, L. Seidman, and J. Roger (2014), Quantifying potential earthquake and tsunami hazard in the Lesser Antilles subduction zone of the Caribbean region, *Geophys. J. Int.*, *196*(1), 510–521.

Herring, T. (2003), MATLAB Tools for viewing GPS velocities and time series, *GPS Solutions*, *7*, 194–199, doi:10.1007/s10291-003-0068-0.

Herring, T., R. King, and S. McClusky (2010a), *Gamit and Globk Reference Manuals, Release 10.3*, Mass. Inst. of Technol., Cambridge.

Herring, T., B. King, and S. McClusky (2010b), *Introduction to Gamit/Globk Reference Manual Global Kalman Filter VLBI and GPS Analysis Program. Release 10.3*, Mass. Inst. of Technol., Cambridge.

Heubeck, C., P. Mann, J. Dolan, and S. Monechi (1991), Diachronous uplift and recycling of sedimentary basins during Cenozoic tectonic transpression, northeastern Caribbean plate margin, *Sediment. Geol.*, *70*, 1–32.

Hough, S. E. (2013), Missing great earthquakes, *J. Geophys. Res. Solid Earth*, *118*(3), 1098–1108, doi:10.1002/jgrb.50083.

Hyndman, R. D. (2007), The seismogenic zone of subduction thrust faults, in *The Seismogenic Zone of Subduction thrust faults*, edited by T. Dixon and C. Moore, pp. 15–40, Columbia Univ. Press, New York.

Idarraga-Garia, J., and J. Romero (2010), Neotectonic study of the Santa Marta Fault System, Western foothills of the Sierra Nevada de Santa Marta, Colombia, *J. South Am. Earth Sci.*, *29*(4), 849–860.

Jansma, P. E., G. S. Mattioli, A. Lopez, C. DeMets, T. H. Dixon, P. Mann, and E. Calais (2000), Neotectonics of Puerto Rico and the Virgin Islands, northeastern Caribbean, from GPS geodesy, *Tectonics*, *19*(6), 1021–1037.

Jany, I., K. Scanlon, and A. Mauffret (1990), Geological interpretation of combined Seabeam, GLORIA and seismic data from Anegada Passage (Virgin Islands, north Caribbean), *Mar. Geophys. Res.*, *12*(3), 173–196.

Jouanne, F., F. A. Audemard, C. Beck, A. Van Welden, R. Ollarves, and C. Reinoza (2011), Present-day deformation along the El Pilar fault in eastern Venezuela: Evidence of creep along a major transform boundary, *J. Geodyn.*, *51*(5), 398–410.

Koketsu, K., et al. (2011), A unified source model for the 2011 Tohoku earthquake, *Earth Planet. Sci. Lett.*, *310*(3–4), 480–487.

Kopp, H., et al. (2011), Deep structure of the central Lesser Antilles island arc: Relevance for the formation of continental crust, *Earth Planet. Sci. Lett.*, *304*(1–2), 121–134.

Kroehler, M. E., P. Mann, A. Escalona, and G. Christeson (2011), Late Cretaceous-Miocene diachronous onset of back thrusting along the south Caribbean deformed belt and its importance for understanding processes of arc collision and crustal growth, *Tectonics*, *30*, TC6003, doi:10.1029/2011TC002918.

Ladd, J. W., J. L. Worzel, and J. S. Watkins (1977), Multifold seismic reflection records from the northern Venezuela basin and the north slope of the Muertos trench, in *Island Arcs, Deep Sea Trenches and Back-Arc Basins*, edited by M. Talwani and W. C. Pitman, pp. 41–56, AGU, Washington, D. C.

Laigle, M., et al. (2013), Seismic structure and activity of the north-central Lesser Antilles subduction zone from an integrated approach: Similarities with the Tohoku forearc, *Tectonophysics*, *603*(C), 1–20.

Le Pichon, X., P. Henry, and S. Lallemant (1990), Water flow in the Barbados Accretionary Complex, *J. Geophys. Res.*, *95*(B), 8945–8967.

Leroy, S., and A. Mauffret (1996), Intraplate deformation in the Caribbean region, *J. Geodyn.*, *21*(1), 113–122.

Lopez, A., S. Stein, T. Dixon, G. Sella, E. Calais, P. Jansma, J. Weber, and P. LaFemina (2006), Is there a northern Lesser Antilles forearc block?, *Geophys. Res. Lett.*, *33*, L07313, doi:10.1029/2005GL025293.

Loveless, J. P., and B. J. Meade (2010), Geodetic imaging of plate motions, slip rates, and partitioning of deformation in Japan, *J. Geophys. Res.*, *115*, B02410, doi:10.1029/2008JB006248.

Manaker, D. M., E. Calais, A. M. Freed, S. T. Ali, P. Przybylski, G. S. Mattioli, P. Jansma, C. Prépetit, and J. B. De Chabalier (2008), Interseismic plate coupling and strain partitioning in the northeastern Caribbean, *Geophys. J. Int.*, *174*(3), 889–903.

Manga, M., et al. (2012), Heat flow in the Lesser Antilles island arc and adjacent back arc Grenada basin, *Geochem. Geophys. Geosyst.*, *13*, Q08007, doi:10.1029/2012GC004260.

Mann, P., C. Schubert, and K. Burke (1990), Review of caribbean neotectonics, in *The Caribbean Region: Geological Society of America*, edited by G. Dengo and J. E. Case, pp. 307–338, The Geology of North America. Research supported by Univ. of Texas, CONICIT, and Universidad de Los Andes, Boulder, Colo.

Mann, P., F. Taylor, R. L. Edwards, and T.-L. Ku (1995), Actively evolving microplate formation by oblique collision and sideways motion along strike-slip faults: An example from the northeastern Caribbean plate margin, *Tectonophysics*, *246*(1), 1–69.

Mann, P., E. Calais, J.-C. Ruegg, C. DeMets, P. E. Jansma, and G. S. Mattioli (2002), Oblique collision in the northeastern Caribbean from GPS measurements and geological observations, *Tectonics*, *21*(6), 1058, doi:10.1029/2001TC001363.

Masson, D., and K. M. Scanlon (1991), The neotectonic setting of Puerto Rico, *Geol. Soc. Am. Bull.*, *103*(1), 144–154.

Mauffret, A., and S. Leroy (1999), Neogene intraplate deformation of the Caribbean plate at the Beata Ridge, *Sediment. Basins World*, *4*, 627–669.

Mazzotti, S., X. Le Pichon, P. Henry, and S. -I. Miyazaki (2000), Full interseismic locking of the Nankai and Japan-West Kurile subduction zones: An analysis of uniform elastic strain accumulation in Japan constrained by permanent GPS, *J. Geophys. Res.*, *105*(B6), 13,159–13,177.

McCaffrey, R. (2002), Crustal block rotations and plate coupling, in *Plate Boundary Zones*, edited by S. Stein and J. Freymueller, pp. 101–122, AGU, Washington, D. C.

McCaffrey, R., L. M. Wallace, and J. Beavan (2008), Slow slip and frictional transition at low temperature at the Hikurangi subduction zone, *Nat. Geosci.*, *1*(5), 316–320.

McCann, W. R. (2006), Estimating the threat of tsunamogenic earthquakes and earthquake induced-landslide tsunami in the Caribbean, *paper presented at NSF Caribbean Tsunami WOrkshop*, World Scientific, San Juan, Puerto Rico.

McCann, W. R., and L. R. Sykes (1984a), Subduction of aseismic ridges beneath the Caribbean plate: Implications for the tectonics and seismic potential of the northeastern Caribbean, *J. Geophys. Res.*, *89*(B6), 4493–4519.

McCann, W. R., and L. R. Sykes (1984b), Subduction of aseismic ridges beneath the Caribbean plate: Implications for the tectonics and seismic potential of the northeastern Caribbean, *J. Geophys. Res.*, *89*(B6), 4493–4519.

McCann, W. R., J. W. Dewey, A. J. Murphy, and S. T. Harding (1982), A large normal-fault earthquake in the overriding wedge of the Lesser Antilles subduction zone: The earthquake of 8 October 1974, *Bull. Seismol. Soc. Am.*, *72*(6A), 2267–2283.

Meade, B. J., and J. P. Loveless (2009), Block modeling with connected fault-network geometries and a linear elastic coupling estimator in spherical coordinates, *Bull. Seismol. Soc. Am.*, *99*(6), 3124–3139.

Meade, B. J., B. H. Hager, S. C. McClusky, R. E. Reilinger, S. Ergintav, O. Lenk, A. Barka, and H. Özener (2002), Estimates of seismic potential in the Marmara Sea region from block models of secular deformation constrained by Global Positioning System measurements, *Bull. Seismol. Soc. Am.*, *92*(1), 208–215.

Mendoza, C. (2000), Rupture history of the 1997 Cariaco, Venezuela, earthquake from teleseismic P waves, *Geophys. Res. Lett.*, *27*(10), 1555–1558.

Miller, M. S., A. Levander, F. Niu, and A. Li (2009), Upper mantle structure beneath the Caribbean-South American plate boundary from surface wave tomography, *J. Geophys. Res.*, *114*, B01312, doi:10.1029/2007JB005507.

Mondziel, S., N. Grindlay, P. Mann, A. Escalona, and L. Abrams (2010), Morphology, structure, and tectonic evolution of the Mona Canyon (northern mona passage) from multibeam bathymetry, sidescan sonar, and seismic reflection profiles, *Tectonics*, *29*, TC2003, doi:10.1029/2008TC002441.

Müller, D., and W. Smith (1993), Deformation of the oceanic crust between the North American and South American plates, *J. Geophys. Res.*, *98*(B5), 8275–8291, doi:10.1029/92JB02863.

Nocquet, J., et al. (2014), Motion of continental slivers and creeping subduction in the Northern Andes, *Nat. Geosci.*, *7*(4), 287–291.

Okada, Y. (1985), Surface deformation due to shear and tensile faults in a half-space, *Bull. Seismol. Soc. Am.*, *75*(4), 1135–1154.

Paris, G., M. Machette, R. Dart, and K. Haller (2000), Map and database of quaternary faults and folds in Colombia and its offshore regions, *USGS Open-File Rep. 00-0284*, U.S. Geol. Surv., Reston, Va.

Patriat, M., T. Pichot, G. K. Westbrook, M. Umber, E. Deville, F. Benard, W. R. Roest, B. Loubrieu, and the ANTIPLAC Cruise Party (2011), Evidence for Quaternary convergence across the North America-South America plate boundary zone, east of the Lesser Antilles, *Geology*, *39*(10), 979–982.

Pérez, O. J., R. Bilham, R. Bendick, J. R. Velandia, N. Hernández, C. Moncayo, M. Hoyer, and M. Kozuch (2001), Velocity field across the Southern Caribbean plate boundary and estimates of Caribbean/South-American plate motion using GPS geodesy 1994–2000, *Geophys. Res. Lett.*, *28*(15), 2987–2990.

Perez, O. J., et al. (2011), GPS derived velocity field in western Venezuela: Dextral shear component associated to the Boconó fault and convergent component normal to the Andes, *Interciencia*, *36*(1), 39–44.

Perrot, J., E. Calais, and B. M. de (1997), Tectonic and kinematic regime along the northern Caribbean plate boundary: New insights from broad-band modeling of the May 25, 1992, $Ms = 6.9$ Cabo Cruz, Cuba, earthquake, *Pure and Appl Geophys.*, *149*(3), 475–487.

Petit, G., and B. Luzum (2010), IERS conventions, *Tech. Rep.*, DTIC DocumentAUTHOR: Please provide location for reference "Petit and Luzum, 2010".

Pichot, T., et al. (2012), The cenozoic tectonostratigraphic evolution of the Barracuda Ridge and Tiburon Rise, at the western end of the North America-South America plate boundary zone, *Mar. Geol.*, *303*, 154–171.

Prentice, C. S., P. Mann, L. R. Peña, and G. Burr (2003), Slip rate and earthquake recurrence along the central septentrional fault, North American-Caribbean plate boundary, Dominican Republic, *J. Geophys. Res.*, *108*(B3), 2149, doi:10.1029/2001JB000442.

Prentice, C. S., J. C. Weber, C. J. Crosby, and D. Ragona (2010), Prehistoric earthquakes on the Caribbean-South American plate boundary, central range fault, Trinidad, *Geology*, *38*(8), 675–678.

Pubellier, M., A. Mauffret, S. Leroy, J. M. Vila, and H. Amilcar (2000), Plate boundary readjustment in oblique convergence: Example of the Neogene of Hispaniola, Greater Antilles, *Tectonics*, *19*(4), 630–648.

Reilinger, R., et al. (2006a), GPS constraints on continental deformation in the Africa-Arabia-Eurasia continental collision zone and implications for the dynamics of plate interactions, *J. Geophys. Res.*, *111*, B05411, doi:10.1029/2005JB004051.

Reilinger, R., et al. (2006b), GPS constraints on continental deformation in the Africa-Arabia-Eurasia continental collision zone and implications for the dynamics of plate interactions, *J. Geophys. Res.*, *111*, B05411, doi:10.1029/2005JB004051.

Robson, G. (1964), An earthquake catalogue for the eastern Caribbean 1530–1960, *Bull. Seismol. Soc. Am.*, *54*(2), 785–832.

Roest, W., and B. Collette (1986), The fifteen twenty fracture zone and the North American-South American plate boundary, *J. Geol. Soc.*, *143*(5), 833–843.

Rosencrantz, E., and P. Mann (1991), Seamarc II mapping of transform faults in the Cayman trough, Caribbean Sea, *Geology*, *19*(7), 690–693.

Rosencrantz, E., M. I. Ross, and J. G. Sclater (1988), Age and spreading history of the Cayman trough as determined from depth, heat flow, and magnetic anomalies, *J. Geophys. Res.*, *93*(B3), 2141–2157.

Ruff, L., and H. Kanamori (1980), Seismicity and the subduction process, *Phys. Earth Planet. Inter.*, *23*(3), 240–252.

Sanchez-Rojas, J., and M. Palma (2014), Crustal density structure in northwestern South America derived from analysis and 3-D modeling of gravity and seismicity data, *Tectonophysics*, *634*, 97–115.

Sandwell, D. T., and W. H. Smith (2009), Global marine gravity from retracted Geosat and ERS-1 altimetry: Ridge Segmentation versus spreading rate, *J. Geophys. Res.*, *114*, B01411, doi:10.1029/2008JB006008.

Saria, E., E. Calais, D. Stamps, D. Delvaux, and C. Hartnady (2014), Present-day kinematics of the East African rift, *J. Geophys. Res. Solid Earth*, *119*(4), 3584–3600, doi:10.1002/2013JB010901.

Savage, J. (1983), A dislocation model of strain accumulation and release at a subduction zone, *J. Geophys. Res.*, *88*(B6), 4984–4996.

Scherer, J. (1912), Great earthquakes in the island of Haiti, *Bull. Seismol. Soc. Am.*, *2*(3), 161–180.

Schmid, R., P. Steigenberger, G. Gendt, M. Ge, and M. Rothacher (2007), Generation of a consistent absolute phase-center correction model for GPS receiver and satellite antennas, *J. Geod.*, *81*(12), 781–798.

Scholz, C. H., and J. Campos (1995), On the mechanism of seismic decoupling and back-arc spreading at subduction zones, *J. Geophys. Res.*, *100*(B11), 22,103–22,115.

Schubert, C. (1982), Neotectonics of Boconó fault, western Venezuela, *Tectonophysics*, *85*(3), 205–220.

Soto, M., P. Mann, A. Escalona, and L. Wood (2007), Late holocene strike-slip offset of a subsurface channel interpreted from three-dimensional seismic data, Eastern Offshore Trinidad, *Geology*, *35*, 859–862.

Stein, S., J. F. Engeln, D. A. Wiens, K. Fujita, and R. C. Speed (1982), Subduction seismicity and tectonics in the Lesser Antilles arc, *J. Geophys. Res*, *87*(NB10), 8642–8664.

Sykes, L. R., W. R. McCann, and A. L. Kafka (1982), Motion of Caribbean plate during last 7 million years and implications for earlier Cenozoic movements, *J. Geophys. Res.*, *87*(B13), 10,656–10,676.

ten Brink, U., and J. Lin (2004), Stress interaction between subduction earthquakes and forearc strikeslip faults: Modeling and application to the northern Caribbean plate boundary, *J. Geophys. Res.*, *109*, B12310, doi:10.1029/2004JB003031.

ten Brink, U., W. Danforth, C. Polloni, B. Andrews, P. Llanes, S. Smith, E. Parker, and T. Uozumi (2004), New seafloor map of the Puerto Rico trench helps assess earthquake and tsunami hazards, *Eos Trans. AGU*, *85*(37), 349–354, doi:10.1029/2004EO370001.

ten Brink, U. S., W. H. Bakun, and C. H. Flores (2011), Historical perspective on seismic hazard to Hispaniola and the northeast Caribbean region, *J. Geophys. Res.*, *116*, B12318, doi:10.1029/2011JB008497.

Trenkamp, R., J. N. Kellogg, J. T. Freymueller, and H. P. Mora (2002), Wide plate margin deformation, southern Central America and northwestern South America, casa GPS observations, *J. South Am. Earth Sci.*, *15*(2), 157–171.

Van Dusen, S. R., and D. I. Doser (2000), Faulting processes of historic (1917–1962) M 6.0 earthquakes along the North-Central Caribbean margin, *Pure Appl. Geophys.*, *157*(5), 719–736.

Vernant, P., R. Reilinger, and S. McClusky (2014), Geodetic evidence for low coupling on the Hellenic subduction plate interface, *Earth Planet. Sci. Lett.*, *385*, 122–129.

Wallace, L. M., P. Barnes, J. Beavan, R. Van Dissen, N. Litchfield, J. Mountjoy, R. Langridge, G. Lamarche, and N. Pondard (2012a), The kinematics of a transition from subduction to strike-slip: An example from the central New Zealand plate boundary, *J. Geophys. Res.*, *117*, B02405, doi:10.1029/2011JB008640.

Wallace, L. M., Å. Fagereng, and S. Ellis (2012b), Upper plate tectonic stress state may influence interseismic coupling on subduction megathrusts, *Geology*, *40*(10), 895–898.

Weber, J. C., et al. (2001), GPS estimate of relative motion between the Caribbean and South American plates, and geologic implications for Trinidad and Venezuela, *Geology*, *29*(1), 75–78.

Weber, J. C., J. Saleh, S. Balkaransingh, T. Dixon, W. Ambeh, T. Leong, A. Rodriguez, and K. Miller (2010), Triangulation-to-GPS and GPS-to-GPS geodesy in Trinidad, West Indies: Neotectonics, seismic risk, and geologic implications, *Mar. Pet. Geol.*, *28*(1), 200–211.

Wells, D. L., and K. J. Coppersmith (1994), New empirical relationships among magnitude, rupture length, rupture width, rupture area, and surface displacement, *Bull. Seismol. Soc. Am.*, *84*(4), 974–1002.

Wessel, P., and W. H. Smith (1998), New, improved version of Generic Mapping Tools released, *Eos. Trans. AGU*, *79*(47), 579–579.

White, S. M., R. Trenkamp, and J. N. Kellogg (2003), Recent crustal deformation and the earthquake cycle along the Ecuador-Colombia subduction zone, *Earth Planet. Sci. Lett.*, *216*(3), 231–242.

Wiggins-Grandison, M. D. (2004), Simultaneous inversion for local earthquake hypocentres, station corrections and 1-D velocity model of the Jamaican crust, *Earth Planet. Sci. Lett.*, *224*(1), 229–240.